Authors response to Referee #1

We thank Referee #1 for the feedback provided. All the comments and the suggestions were useful to improve the quality and the readability of the paper. Detailed responses to each comment are given below together with the changes that will be done in the revised version of the manuscript. RC indicates the referee comments, AC the authors comments. To help referees to visualize the changes that will be done in the revised version of the manuscript we reported both the original manuscript's text and the authors changes to the manuscript.

RC1: Line 31: the two question marks should be deleted

AC: it's a mistake due to a missing reference.

Original manuscript: Meteorological drought is related to precipitation shortages; hydrological drought refers to periods of precipitation shortfall on surface or subsurface water supply ??, while agricultural drought is conventionally linked to soil moisture deficit.

Author's changes to the manuscript (Lines 31-32): Meteorological drought is related to precipitation shortages; hydrological drought refers to periods of precipitation shortfall on surface or subsurface water supply (Sheffield & Wood, 2011) while agricultural drought is conventionally linked to soil moisture deficit.

RC1: Line 248-251: The authors should explain why they used the Spearman correlation instead of the most common Pearson correlation coefficient. Of course, there is a reference concerning this subject (Wedgbrow et al., 2002) but this obliges the reader to find the reference in order to be informed.

AC: We have reconsidered the use of the Pearson correlation coefficient instead of Spearman. In fact, the use of the Pearson correlation coefficient could be preferable when dealing with normal variables. Therefore, the Spearman correlation coefficient has been substituted with the Pearson correlation coefficient. The manuscript will be changed accordingly.

Original manuscript: While in the majority of the papers the Pearson correlation coefficient was employed, in the present study the Spearman correlation coefficient was preferred as a measure of the statistical relationship between the indices, as suggested in (Wedgbrow et al., 2002). The number of significant correlations at 5% and 1% was evaluated for four SPI aggregation timescales (Table 8). The highest number of significant correlations was found in the cases of SPI2 and SPI3, which exhibit very similar performances at 1% significant level. This finding is in agreement with previous studies such as (Hongshuo et al., 2014) that found that VHI and SPI3 have the highest correlation for croplands, whereas VHI and 6-month SPI have the highest correlation for forest in the Southwest of China; and (Ma'rufah, 2017) that found that significant correlation coefficient values on SPI3 and VHI are common in the southern part of Indonesia. Since SPI3 has been used in literature and the percentage of significant correlation at 1% level is relevant, it has been decided to aggregate SPI over a 3 months period and use SPI3 in the following discussion.

Table 8: Number of significant correlations between VHI and various SPI aggregation timescales. Value is expressed as percentage evaluated with respect to the total number of grid cells (987).

	% significant correlations 5%	% significant correlations 1%
SPI1	94.53	90.78
SPI2	97.26	95.44
SPI3	96.66	95.34
SPI6	89.77	85.61

Author's changes to the manuscript (Lines 248-259): The Pearson correlation coefficient was employed in the present study as a measure of the statistical relationship between the indices. The number of significant correlations at 5% and 1% was evaluated for four SPI aggregation timescales (Table 8). The highest number of significant correlations was found in the cases of SPI2 and SPI3, which exhibit very similar performances at 1% significant level. This finding is in agreement with previous studies such as (Hongshuo et al., 2014) that found that VHI and SPI3 have the highest correlation for croplands, whereas VHI and 6-month SPI have the highest correlation for forest in the Southwest of China; and (Ma'rufah, 2017) that found that significant correlation coefficient values on SPI3 and VHI are common in the southern part of Indonesia. Since SPI3 has been used in literature and the percentage of significant correlation at 1% level is relevant, it has been decided to aggregate SPI over a 3 months period and use SPI3 in the following discussion.

Table 8: Number of significant correlations (Pearson correlation coefficient) between VHI and various SPI aggregation timescales. Value is expressed as percentage evaluated with respect to the total number of grid cells (987).

	% significant correlations 5%	% significant correlations 1%
SPI1	93.52	91.29
SPI2	96.76	95.34
SPI3	96.15	94.83
SPI6	90.07	85.82

RC1: Line 300-301: "It's clear from Fig.6 that PPVI identified the reported drought events better than SPI3 and VHI. AUC was 0.828 for PPVI, 0.740 for SPI3 and 0.784 for VHI." We cannot observe the values 0.828 for PPVI, 0.740 for SPI3 and 0.784 for VHI referred in the figures.

AC: The sentence can be rephrased, and the Figure 6 can be adjusted as follows.

Original manuscript: It's clear from Fig.6 that PPVI identified the reported drought events better than SPI3 and VHI. AUC was 0.828 for PPVI, 0.740 for SPI3 and 0.784 for VHI.

Author's changes to the manuscript (Lines 300-304): It's clear from Fig. 6 that the red curve, representing PPVI, is the furthest from the diagonal line in all the panels of the figure. The Area Under the Curve (AUC) was used as criteria to establish which index gave the best performances. AUC values are shown in Fig. 6 for each index and various configurations of the model.
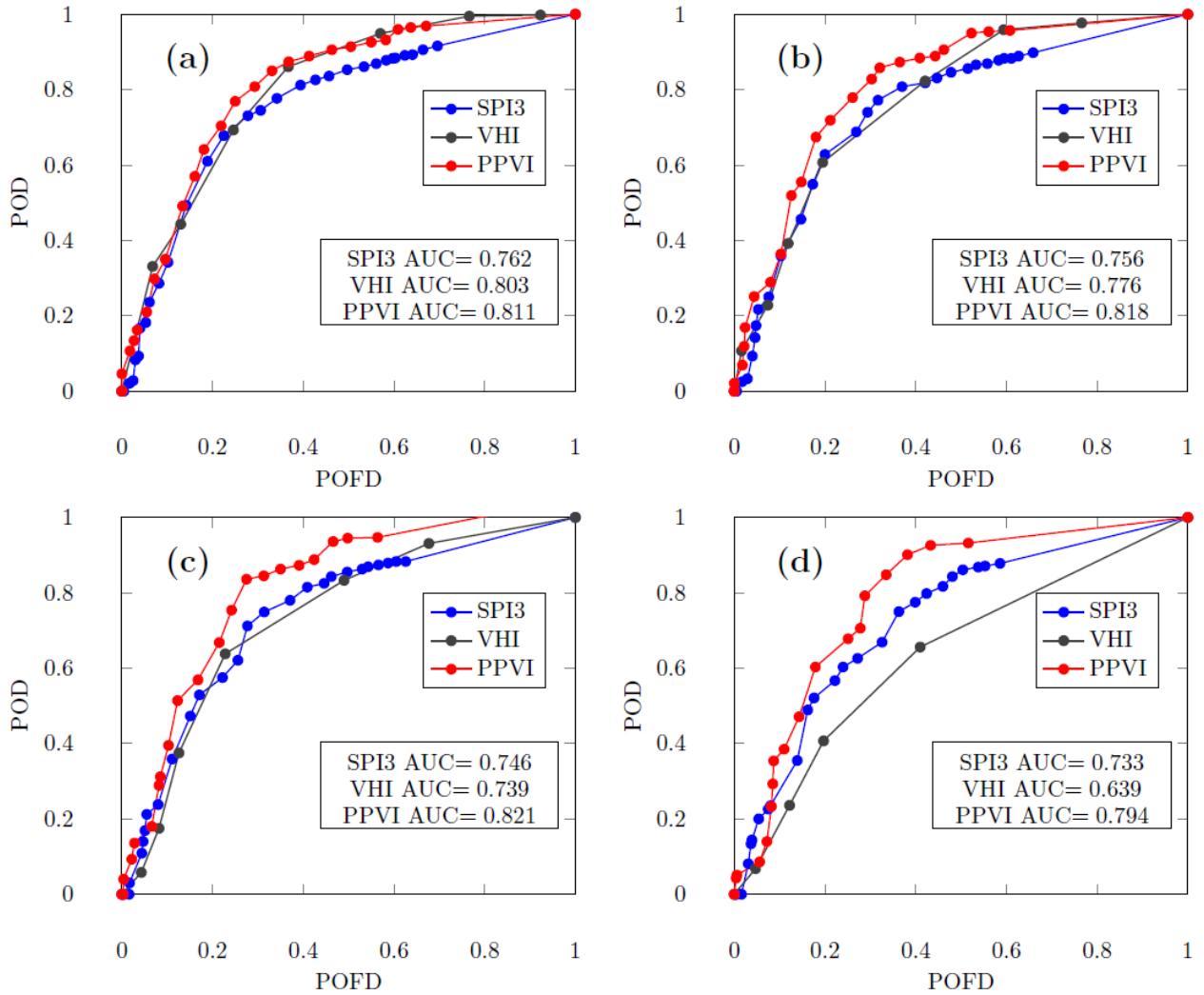
Figure 6: Comparison among the performances of SPI3, VHI and PPVI in identifying reported drought events; thresholds Z, Z_S and Z_V are varying, $z = -1.1$, $z_s = 0$ and $z_v = 40$; n = 80 and four cases for N are shown: (a): N = 10%; (b): N = 20%; (c):N = 30% and (d): N=50%.

RC1: Lines 326-328: 'Short-term droughts are often not reported in text-based documents, and information on drought start and end date were retrieved from documents that mainly described the impacts related to drought. PPVI showed a good agreement with reported information in identifying the areas of the country hit by the drought.' In Fig. 7, in the 'Observation' sub-figure, no department is highlighted in red. Does this mean that no drought was observed, or is this a mistake? In the former case, the authors should comment on this situation. In Figures 7 to 9 there is a comparison of indices and 'Observation' concerning the various departments of Haiti. Please define the criteria according to which a department is highlighted in red (drought conditions). Table 11. 'Reported as drought': Define the criteria of this classification.

AC: In Fig.7 no department was highlighted in red since no drought was observed during that week according to text-based documents regarding droughts in Haiti. Departments are highlighted in red if, according to the documents cited in Table 7, drought was observed during that week in the department. The same criteria were adopted in Table 11 to establish if, according to observations, a department was in drought.

Figure 7, 8 and 9 will be modified to include a legend to clearly distinguish between departments in drought and departments not in drought. A description of the criteria used to define drought according to observation

will be given. The text of the manuscript will be modified to clarify the criteria adopted to identify drought in the various departments.

Author's changes to the manuscript: (Lines 310 – 319): At first, week 45 of 1995 was considered. No drought events were reported in that period according to the information available in the analysed documents (see Table7). Figure 7 shows that, while SPI3 identified all the southern part of the country as dry areas and VHI showed vegetation suffering in two departments (Centre and West), PPVI did not show signs of drought, except for a minor number of grid cells. Figure 8 shows that in 2015, when the whole country was reported to be in severe drought conditions (see Table 7 and (NOAA, 2017; OXFAM & Action conte la Faim, 2015)), PPVI captured well the pattern, only a few grid cells were not in drought conditions. The SPI3 was also able to catch the situation, while for the VHI only 58% of the county was in drought. During week 8 of 2012, only the Northern part of the country was in drought (Fig. 9), as highlighted by (USAID & FEWSNET, 2012) (see Table 7). Five departments were reported to be stressed (North, North West, North East, Artibonite, Centre, see Table 7). All the three indices showed the North West as the department most affected by drought when considering the percentage of the department area hit by the drought. PPVI then classified Artibonite, North, Centre and North East, while SPI3 as second and third most affected departments identified South and Grand Anse and VHI Centre and Nippes (Table 11).
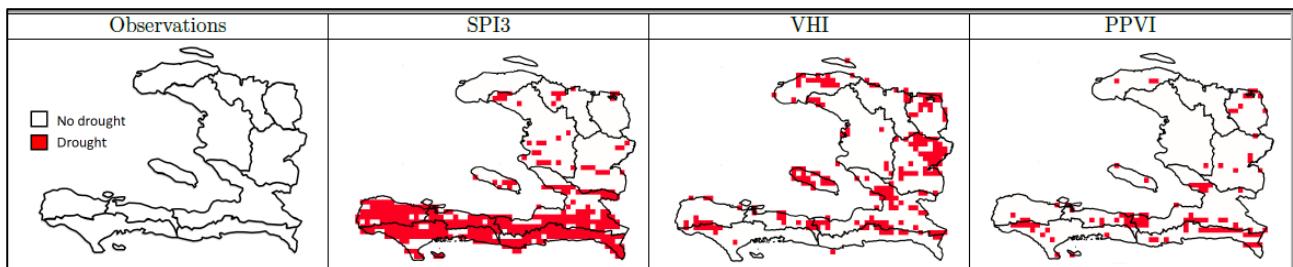

Figure 7: Comparison of the performance of SPI3, VHI, and PPVI in identifying the areas hit by drought. Week 45 of 1995. Departments highlighted in red are the ones in drought according to observations (Table 7), red cells are the ones in drought condition according to the various indices.
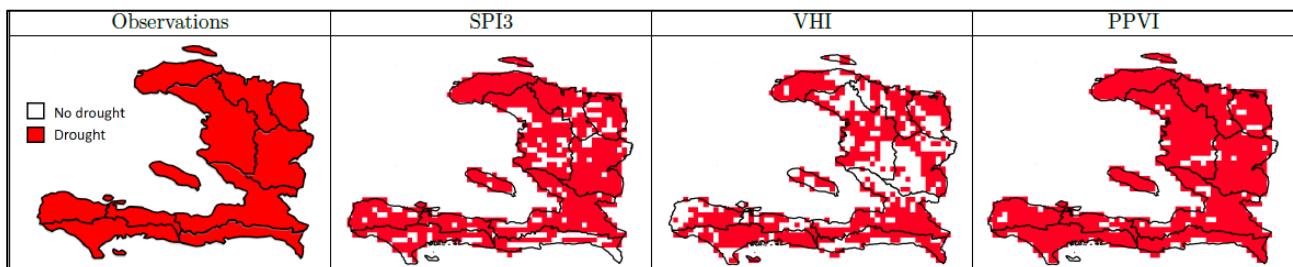
Figure 8: Same as Fig. 7 but for week 33 of 2015. Departments highlighted in red are the ones in drought according to observations, red cells are the ones in drought condition according to the various indices.
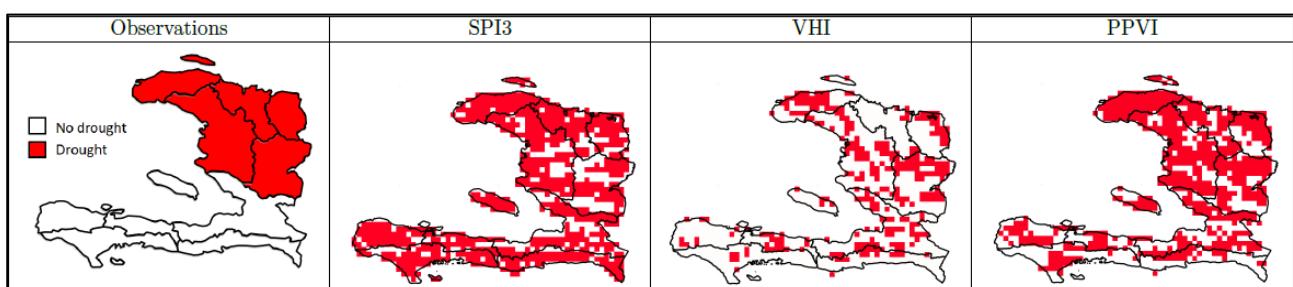

Figure 9: Same as Fig. 7 but for week 8 of 2012. Departments highlighted in red are the ones in drought according to observations, red cells are the ones in drought condition according to the various indices.

Table 11. Performance of PPVI, SPI3, and VHI in identifying departments hit by drought during week 8 of 2012 and comparison with observations. Observations are retrieved from the text-based documents reported in Table 7.

		% of the area			Ranking of affected departments		
Department	Reported as in drought	PPVI	SPI3	VHI	PPVI	SPI3	VHI
North West	Yes	93.1	91.7	47.2	1	1	1
Artibonite	Yes	75.1	72.8	34.1	2	7	5
North	Yes	74.6	82.1	10.4	3	4	9
Centre	Yes	67.2	54.3	45.7	4	10	2
North East	Yes	62.1	72.4	34.5	5	8	4
West	No	61.8	72.1	32.7	6	9	6
Nippes	No	51.2	75.6	36.6	7	5	3
Grand Anse	No	47.8	82.1	10.4	8	3	8
South	No	32.6	75.3	9	9	6	10
South East	No	30.8	84.6	20	10	2	7

RC1: A comparison of PPVI performances to the ones of other composite indices, would be a considerable improvement.

AC: As already discussed in the manuscript (lines 365-368), a comparison with other composite indices is hard, due to the unavailability of composite indices with the same characteristics of PPVI. In fact, previous composite indices do not include both the meteorological and the agricultural aspect of drought or are not available globally or cannot be computed with only remote sensing datasets. In addition, VHI is already a composite drought index since it is derived from the linear combination of TCI and VCI. Therefore, in the manuscript, a comparison of PPVI performance with respect to the ones of a composite drought index was already performed.

References:

Bonaccorso, B., Cancelliere, A., & Rossi, G. (2015). Probabilistic forecasting of drought class transitions in Sicily (Italy) using Standardized Precipitation Index and North Atlantic Oscillation Index. *Journal of Hydrology*, *526*, 136–150. https://doi.org/10.1016/j.jhydrol.2015.01.070

Hongshuo, W., Hui, L., & Desheng, L. (2014). Remotely sensed drought index and its responses to meteorological drought in Southwest China. *Remote Sensing Letters*, *5*.

Ma'rufah, U. (2017). Analysis of relationship between meteorological and agricultural drought using standardized precipitation index and vegetation health index Analysis of relationship between meteorological and agricultural drought using standardized precipitation index and. *Earth and Environmental Science*, *54*, 7. https://doi.org/10.1088/1742-6596/755/1/011001

NOAA. (2017). *Climate Prediction Center ' s Hispaniola Hazards Outlook* (p. 3424).

OXFAM, & Action conte la Faim. (2015). *Etat des lieux de la situation de secheresse dans le department du Nord Ouest et dans le Haut Artibonite*.

Sheffield, J., & Wood, E. F. (2011). *Drought: past problems and future scenarios*. Routledge.

USAID, & FEWSNET. (2012). *Climate Prediction Center ' s Hispaniola Hazards Outlook For USAID / FEWS-NET* (p. 8000).

Wedgbrow, C. S., Wilby, R. L., & Fox, H. R. (2002). *PROSPECTS FOR SEASONAL FORECASTING OF SUMMER DROUGHT*. *236*, 219–236. https://doi.org/10.1002/joc.735

We would like to thank Referee #2 for the insightful comments on the paper. Detailed responses to each comment are given below together with the changes that will be done in the revised version of the manuscript. RC indicates the referee comments, AC the authors comments. To help referees to visualize the changes that will be done in the revised version of the manuscript we reported both the original manuscript's text and the authors changes to the manuscript.

RC2: Use of CHIRP dataset instead of the CHIRPS dataset. Please justify why the CHIRP dataset is used for the study area. Based on the study of Funk el al., 2015 it is proved that constraining the CHIRP by the CHPclim reduces systematic errors and the CHIRPS dataset produces low MAE and bias statistic than the CHIRP dataset.

AC: The authors are aware of the biases in the CHIRP dataset, but they aim at proposing an index for drought monitoring in near-real time; therefore, they selected the product with the shortest latency time. The main reason for using CHIRP instead of CHIRPS is the reduced latency time of the first dataset. In fact, as reported by (Funk et al., 2015), CHIRPS latency time is about three weeks; a preliminary version of CHIRPS with a 2-day latency time is available for GTS and Mexico only. In the case of CHIRP, latency time is about 2 days, and the product is available all over the world. CHIRP latency time can be checked at (Climate Hazard Group, 2015) by looking at the availability of the images.

Original manuscript: The use of CHIRP instead of CHIRPS (the Climate Hazard Group Infrared Precipitation with Stations) is related to the data latency time, which is shorter in the case of CHIRP since it doesn't include data from weather stations.

Author's changes to the manuscript (lines 107-111): The use of CHIRP instead of CHIRPS (the Climate Hazard Group Infrared Precipitation with Stations) is related to the data latency time. Since the aim of the work is the development of an index for near-real time drought monitoring, the product with the shortest latency time was selected. CHIRPS data have a latency time of about three weeks (Funk et al., 2015), while CHIRP's latency is about 2 days, as can be checked on the dataset website (Climate Hazard Group, 2015)

RC2: It would be interesting to see a comparison of the observed precipitation pattern with the used rainfall dataset. How close is the used dataset with the observed rainfall in Haiti? Please, provide scientific evidence in the revised manuscript which demonstrates the superiority of the used dataset when compared with the CHIRPS dataset for spatial and temporal (monthly) rainfall modelling at the study area.

AC: Unfortunately, as highlighted by (Mari et al., 2015) "Systematic collection of rainfall through rain gauges has been relatively rare in post-earthquake Haiti, with on-the-ground rainfall measurements available only for Ouest (by USGS) and Sud (by Haiti Regeneration Initiative) departments". A map of existing rain gauges in Haiti reported in Eisenberg et al. (2013) shows the presence of only 5 gauges all over the country recording for a short period of time. Thus, a comparison between observed precipitation and rainfall retrieved from satellite images is not very feasible. The authors tried to overcome the issue providing a comparison with observed drought events, retrieved from text-based documents and international disasters databases, in Section 3.4 of the manuscript.

RC2: Vegetation Health Index: It should be mentioned that all remote sensing indices could be expressed as deviations from the mean using the standardization procedure (i.e. Mckee at al., 1993) as used by Peters et al. [2002]. Hence the adopted classification of VHI using Eq. 1 is a transformation procedure of the typical VHI (from 0 to 1) to a normal distribution using the standardization procedure as proposed by Peters et al.,[2002]. I recommend to the authors to clarify this issue on the revised manuscript and to mention that equal weighting is used for VCI and TCI.

AC: All these comments will be addressed in the revised manuscript as follows.

Original manuscript: The VHI is a remote-sensing index developed to include the effects of temperature on vegetation; in fact, it combines the VCI with the Temperature Condition Index (TCI), which is another remote-sensing index used to determine vegetation stress caused by temperature and excessive wetness. One drawback of the VHI is the impossibility to identify the cause of the vegetation stress; in fact, vegetation can suffer because of various events: excessive wetness, pests, fires, droughts or others. It is a biophysical indicator of a lack of precipitation but can also be seen as representing drought impacts on the ground (Bachmair et al., 2016). It goes from 0, which stands for vegetation in very bad conditions to 100, meaning perfectly healthy vegetation. The classification scheme of VHI, as proposed in (Dalezios et al., 2017) is presented in Table 4.

The VHI is standardized according to the following equation:

$$VHI_{st} = \frac{VHI - \overline{VHI}}{\sigma}$$

where $\overline{VHI}$ is the mean of the distribution and σ its standard deviation. The standardized variable, VHI_{st}, has a distribution with 0 mean and 1 as standard deviation.

Author's changes to the manuscript (lines 134-144): The VHI is a remote-sensing index developed to include the effects of temperature on vegetation; in fact, it combines the VCI with the Temperature Condition Index (TCI) which is another remote-sensing index used to determine vegetation stress caused by temperature and excessive wetness. The VHI is based on a linear combination of VCI and TCI, $VHI = \alpha VCI + (1 - \alpha)TCI$. As suggested by Kogan et al. (2016), when VCI and TCI contributions are not known $\alpha = 0.5$. One drawback of the VHI is the impossibility to identify the cause of the vegetation stress; in fact, vegetation can suffer because of various events: excessive wetness, pests, fires, droughts or others. It is a biophysical indicator of a lack of precipitation but can also be seen as representing drought impacts on the ground (Bachmair et al., 2016). It goes from 0, which stands for vegetation in very bad conditions to 100, meaning perfectly healthy vegetation. The classification scheme of VHI, as proposed in Dalezios et al. (2017), is presented in Table 4.

The VHI is standardized to make comparisons with the SPI easier. As mentioned by Peters et al. (2002), all remote-sensing indices can be expressed as deviations from the mean; therefore, the standardized variable, VHI_{st}, is computed according to the following equation:

$$VHI_{st} = \frac{VHI - \overline{VHI}}{\sigma}$$

Thus, the same procedure proposed in Peters et al. (2002) in the case of the NDVI has been applied to the VHI.

RC2: Furthermore, please discuss why VHI is used using the approach of Kogan and why VHI and TCI are not first standardized and then combined with equal [see also Bento et al., 2018a,b] weighting in a probabilistic form to give the VHI (similar approach to PPVI or the approach of multivariate distributions using parametric [Hao and AgaKouchack, 2013] or a non-parametric approaches [Hao and AgaKouchack, 2014]

AC: The VHI as proposed by Kogan was used since it is a consolidated product, already applied to monitor vegetation health in various studies concerning different topics such as food security (Kogan, 2019), insurance (Bokusheva et al., 2016) and drought identification (Pei et al., 2018; Sholihah et al., 2016). As above mentioned, the VHI was standardized to facilitate the interpretation of the index inside the bivariate context. PPVI values do not change if PPVI is computed by combining SPI3 and non-standardized VHI through the bivariate normal distribution function (see panel (a) of Fig. 1). In addition, the authors computed VHI_{st} by a

linear combination of standardized TCI (TCI_{st}) and standardized VCI (VCI_{st}), applying equal weighting of the two indices, with TCI_{st} and VCI_{st} computed according to Peters et al. (2002). PPVI values do not change, as shown in panel (b) of Figure 1.
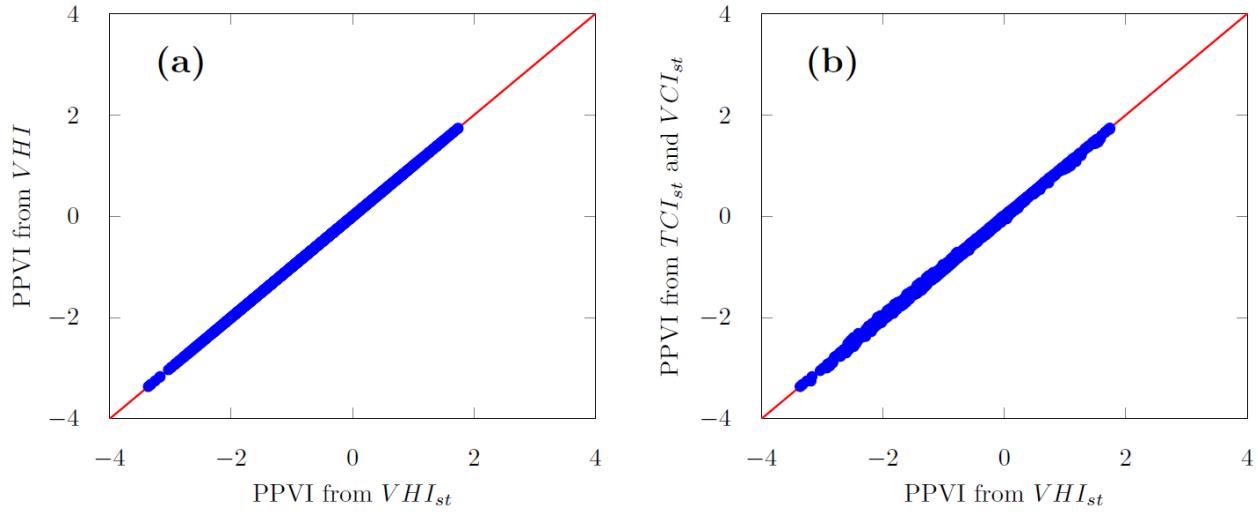

Figure 1: (a): relationship between PPVI computed from VHI_{st} and PPVI computed from VHI; (b): relationship between PPVI computed from VHI_{st} and PPVI computed from VHI_{st} retrieved from linear combination of VCI_{st} and TCI_{st}.

RC2: Comparison with identified drought events. Is it possible to include a section with a comparison of PPVI with historical identified drought events? This comparison could exemplify the proposed index and strengthen the scientific quality of the manuscript.

AC: The comparison with identified drought events, reported in Table 7 of the original manuscript and identified from text-based documents such as governmental reports and international disaster databases, is already reported in the manuscript in Section 3.4, "Indices comparison", where PPVI performance in reproducing observed drought events is compared with SPI3 and VHI performance. To make the manuscript clearer on this aspect, Section 3.4 "Indices comparison" will be renamed in "Comparison of drought indices with observed drought events". In addition, Figure 2 will be added in Section 3.4 (as Figure 7 in the revised manuscript) to allow an easy comparison between drought indices performance in identifying observed drought events.
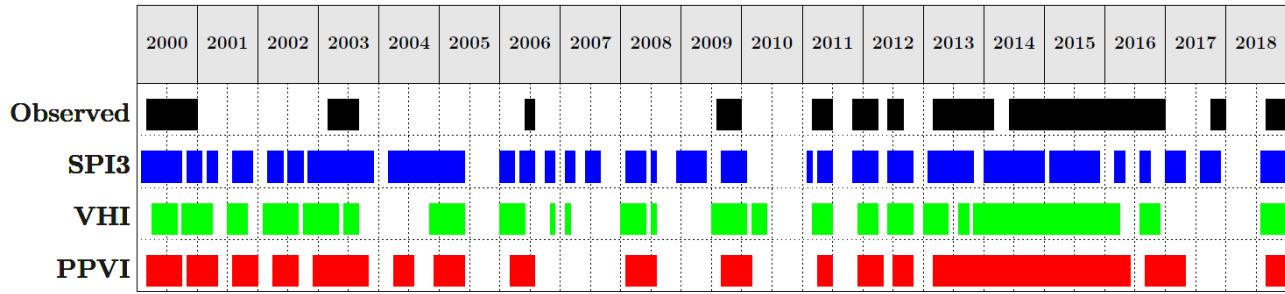

Figure 2: comparison between observed drought events and drought events identified by PPVI, SPI3 and VHI when calibrated with the best performing parameters shown in Table 10. The comparison is shown for the period from 2000 to 2018.

Table 10 will be modified to show the best performing parameters not only for PPVI but for all the three indices.

Table 10: Best configuration parameters for the model when applied with PPVI, SPI3 and VHI.

	Z	z	N	n	TN	FP	FN	TP	POFD	POD

PPVI	-1.8	-1.1	30%	8%	957	379	99	506	0.284	0.836
SPI3	-1.3	0	20%	8%	943	393	157	448	0.294	0.740
VHI	22	40	10%	8%	935	401	150	455	0.300	0.752

References:

Bachmair, S., Stahl, K., Collins, K., Hannaford, J., Acreman, M., Svoboda, M., Knutson, C., Smith, K. H., Wall, N., Fuchs, B., Crossman, N. D., & Overton, I. C. (2016). Drought indicators revisited: the need for a wider consideration of environment and society. *Wiley Interdisciplinary Reviews: Water*, *3*(4), 516–536. https://doi.org/10.1002/wat2.1154

Bokusheva, R., Kogan, F., Vitkovskaya, I., Conradt, S., & Batyrbayeva, M. (2016). Agricultural and Forest Meteorology Satellite-based vegetation health indices as a criteria for insuring against drought-related yield losses. *Agricultural and Forest Meteorology*, *220*, 200–206. https://doi.org/10.1016/j.agrformet.2015.12.066

Climate Hazard Group. (2015). *Chirp daily*. ftp://ftp.chg.ucsb.edu/pub/org/chg/products/CHIRP/daily/

Dalezios, N. R., Tarquis, A. M., & Eslamian, S. (2017). Droughts. In N. Dalezios (Ed.), *Environmental Hazards Methodologies for Risk Assessment and Management*. IWA Publishing. https://doi.org/https://doi.org/https://doi.org/10.2166/9781780407135,

Eisenberg, M. C., Kujbida, G., Tuite, A. R., Fisman, D. N., & Tien, J. H. (2013). Examining rainfall and cholera dynamics in Haiti using statistical and dynamic modeling approaches. *Epidemics*, *5*(4), 197–207. https://doi.org/10.1016/j.epidem.2013.09.004

Funk, C., Peterson, P., Landsfeld, M., Pedreros, D., Verdin, J., Shukla, S., Husak, G., Rowland, J., Harrison, L., Hoell, A., & Michaelsen, J. (2015). The climate hazards infrared precipitation with stations - A new environmental record for monitoring extremes. *Scientific Data*, *2*, 1–21. https://doi.org/10.1038/sdata.2015.66

Kogan, F., Guo, W., Strashnaia, A., Kleshenko, A., & Chub, O. (2016). *Modelling and prediction of crop losses from NOAA polar-orbiting operational satellites*. *5705*. https://doi.org/10.1080/19475705.2015.1009178

Kogan, F. N. (2019). Application of Vegetation Health Data and Products for Monitoring Food Security. In *Remote Sensing for Food Security* (pp. 225–241). Springer, Cham. https://doi.org/https://doi.org/10.1007/978-3-319-96256-6_10

Mari, L., Bertuzzo, E., Finger, F., Casagrandi, R., Gatto, M., & Rinaldo, A. (2015). On the predictive ability of mechanistic models for the Haitian cholera epidemic. *Journal of Royal Society Interface*, *12*.

Pei, F., Changjiang, W., Xiaoping, L., Xi, L., Kuiqi, Y., Yi, Z., Kun, W., Li, X., & Gengrui, X. (2018). Monitoring the vegetation activity in China using vegetation health indices. *Agricultural and Forest Meteorology*, *248*, 215–227.

Peters, Al. J., Walter-Shea, E. A., Ji, L., Vina, A., Hayes, M., & Svoboda, M. D. (2002). Drought monitoring with NDVI-based Standardized Vegetation Index. *Photogrammetric Engineering & Remote Sensing*, *68*(1), 71–75.

Sholihah, R. I., Trisasongko, B. H., Shiddiq, D., Ode, L., & Iman, S. (2016). Identification of agricultural drought extent based on vegetation health indices of Landsat data : case of Subang and Karawang , Indonesia. *Procedia Environmental Sciences*, *33*, 14–20. https://doi.org/10.1016/j.proenv.2016.03.051

List of changes made in the manuscript

Line 18: Organizations changed with Organization.

Line 31: "subsurface" has been deleted.

Line 31: question marks have been deleted, a reference has been included.

Line 41: (Gu et al.,2008) changed in Gu et al. (2008).

Line 52: VegDri has been defined.

Line 60: (Serinaldi et al.,2009) and (Bonaccorso et al., 2012) changed in Serinaldi et al. (200) and Bonaccorso et al. (2012).

Line 61: (Shiau et al., 2006) changed in Shiau et al. (2006).

Line 64: (Songbai and Singh, 2010) changed in Songbai and Sing (2010).

Line 70: AMDI-SA has been defined.

Line 79: Temeprature has been corrected.

Lines 108-110: the sentence has been changed according to the answer given to Referee #2.

Line 111: (Funk et al.2015) changed in Funk et al. (2015).

Line 131: (Mckee et al.,1993) changed in Mckee et al. (1993).

Line 137: a sentence has been added to answer Referee #2 comments.

Line 141: (Dalezios et al.2017) changed in Dalezios et al. (2017).

Line 142: a sentence has been added to answer Referee #2 comments.

Line 153: (USDA Risk Management Agency et al., 2006) changed in USDA Risk Management Agency et al. (2006).

Line 157: (Kotz et al., 2000) changed in Kotz et al. (2000).

Line 165: Eq. 3 and Eq. 4 changed in Eqs 3 and 4.

Line 170: (Nelsen, 2006) changed in Nelsen (2006).

Line 189: (Joliffe and Stephenson, 2012) changed in Joliffe and Stephenson (2012).

Line 248: NAO has been defined.

Line 249: (Hongshuo et al., 2014) changed in Hongshuo et al. (2014).

Lines 249-260: The Spearman correlation coefficient has been substituted with the Pearson correlation coefficient. Results have been changed accordingly.

Line 290: Section "Indices comparison" has been renamed into "Comparison of drought indices with observed drought events".

Line 294: a sentence has been changed to address referees' comments.

Lines 301-304: a sentence has been added to address referees' comments.

Line 320: a sentence has been added to describe the newly introduced Figure 7.

Figure 6: AUC values have been corrected.

Figure 7: introduced to answer to the comments of Referee #2.

Figure 8-9-10: Figures have been changed to make them clearer.

Table 8: adjusted to report the number of significant correlations according to the Pearson correlation coefficient instead of the Spearman ones.

Table 10: best performing values for SPI3 and VHI have been added.

Table 11: the caption has been changed to specify the criteria for identifying departments in drought according to historical documents.

A joint probabilistic index for objective drought identification: the case study of Haiti

Beatrice Monteleone[1], Brunella Bonaccorso[2], and Mario Martina[1]

[1]Scuola Universitaria Superiore IUSS Pavia, Pavia, 27100, Italy
[2]Department of Engineering, University of Messina, S. Agata, Messina, 98166, Italy

Correspondence: Beatrice Monteleone (beatrice.monteleone@iusspavia.it)

Abstract. Since drought is a multifaceted phenomenon, more than one variable should be considered for a proper understanding of such extreme event in order to implement adequate risk mitigation strategies such as weather or agricultural indices insurance programs, or disaster risk financing tools. This paper proposes a new composite drought index that accounts for both meteorological and agricultural drought conditions, by combining in a probabilistic framework two consolidated drought indices: the Standardized Precipitation Index (SPI) and the Vegetation Health Index (VHI). The new index, called Probabilistic Precipitation Vegetation Index (PPVI), is scalable, transferable all over the globe and can be updated in near-real time. Furthermore, it is a remote-sensing product, since precipitation are retrieved from satellite and the VHI is a remote-sensing index. In addition, a set of rules to objectively identify drought events is developed and implemented. Both the index and the set of rules have been applied to Haiti. The performance of PPVI has been evaluated by means of the Receiver Operating Characteristics curve and compared to the ones of SPI and VHI considered separately. The new index outperformed SPI and VHI both in drought identification and characterization, thus revealing potential for an effective implementation within drought early warning systems.

1 Introduction

Droughts affect every year an increasing number of people. In the years from 2014 to 2018 more than 70 drought events have been reported all over the world and about 450 million people suffered because of drought-related impacts (CRED, 2017). Due to its complexity, various definitions of the phenomenon have been proposed by different institutions, such as the World Meteorological ~~Organizations~~ Organization (WMO), the Food and Agriculture Organization (FAO) and the United Nations Convention to Combat Desertification (UNCCD). All the institutions focus their attention on a specific aspect of drought: the WMO on the lack of precipitation, the FAO on the decline in crop productivity and the UNCCD on the loss of arable land.

In addition, the quantification of drought effects is a complicated task, since drought impacts are non-structural, widespread over large areas, and of different type and magnitude within the drought-affected area, also depending on economic, social and environmental system vulnerabilities (Wilhite, 2000).

Drought identification through an objective and automatic determination of drought onset, termination and severity allows the timely adoption of appropriate risk management strategies, such as weather index insurance programs (Barnett and Mahul, 2007), agricultural index insurance programs (Jensen and Barrett, 2017), disaster financing (Guimarães Nobre et al., 2019; Linnerooth-Bayer and Hochrainer-Stigler, 2015) and early action planning (Drechsler and Soe, 2016).

Drought features are usually determined through the use of two instruments: indicators, which are variables and parameters used to assess drought conditions (such as precipitation, temperature, and others), and indices, which are numerically computed values from meteorological or hydrological inputs (World Meteorological Organization and Global Water Partnership, 2016). More than 100 indices have been developed by the scientific community (Zargar et al., 2011), each one focusing on a specific aspect of drought (meteorological, hydrological, agricultural and so on). Meteorological drought is related to precipitation shortages; hydrological drought refers to periods of precipitation shortfall on surface ~~or subsurface water supply ??~~ water supply (Sheffield and Wood, 2011), while agricultural drought is conventionally linked to soil moisture deficit. Insufficient soil moisture leads to crop failure and consequent yield reduction; therefore the first economic sector suffering because of drought is agriculture, particularly in those areas where it relies on rainfall. A deeper understanding of agricultural drought dynamics can promote the adoption of risk reduction strategies, such as crop insurance programs.

In recent years various remote-sensing indices have been developed and can be employed in agricultural drought monitoring. The most widespread is the Normalized Difference Vegetation Index (NDVI), which uses NOAA AVHRR satellite data to monitor vegetation greenness (Kogan, 1995a). The main advantages of the NDVI are the very high spatial resolution and the global coverage. The NDVI has already been applied in drought monitoring, such as in ~~(Gu et al., 2008)~~ Gu et al. (2008). Many products were derived from the NDVI, such as the Vegetation Condition Index (VCI), which compares the current NDVI to the range of values observed in the same period in previous years (Liu and Kogan, 1996; Kogan, 1995b) and the Standardized Vegetation Index (SVI), which describes the probability of vegetation condition deviation from normal (Peters et al., 2002). A suite of agricultural drought indices is presented in Table 1.

Since drought is a complex phenomenon, a single index or indicator can be insufficient to fully characterize drought severity and extent. The combination of more than one indicator can be precious to evaluate all the variables involved in drought monitoring, such as precipitation, soil moisture, and streamflow. Over the past 20 years many composite indicators, relying on two or more drought indices or indicators, have been proposed to overcome the issues related to the use of a single variable. Table 2 shows a list of selected composite indices that can be used in agricultural drought monitoring since, in their formulation soil moisture, vegetation condition or variables related to water availability for plants are included.

Multiple methods for taking into account the multivariate behaviour of drought have been explored (Hao and Singh, 2015, 2016). The ~~VegDRI~~ Vegetation Drought Response Index (VegDRI), for example, uses a data mining approach to combine multiple inputs such as the SPI, the NDVI and the Palmer Drought Severity Index (PDSI). A weighted linear combination of the inputs is quite common; it is applied to construct the Composite Drought Indicator (CDI) for Morocco, the Vegetation

Health Index (VHI) and the Objective Blend of Drought Indicators (OBDI). The United States Drought Monitor (USDM) also applies a weighted linear combination of the inputs but adds an expert judgment to define the drought class.

In the last years multiple studies focused the attention on modelling the joint behaviour of two drought characteristics or indices applying bivariate or multivariate statistical approaches. In various cases bivariate distributions are developed by means of copulas as in ~~(Serinaldi et al., 2009) and (Bonaccorso et al., 2012)~~ Serinaldi et al. (2009) and Bonaccorso et al. (2012) , where the joint behaviour of various drought properties is investigated; or in ~~(Shiau, 2006)~~ Shiau (2006) , where two-dimensional copulas are employed to study the joint behaviour of drought duration and severity in Taiwan. ~~(Shiau et al., 2007)~~ Shiau et al. (2007) investigates also the hydrological droughts of the Yellow River in China using a bivariate distribution to model drought duration and severity jointly. Trivariate Plackett copula is used in ~~(Songbai and Singh, 2010)~~ Songbai and Singh (2010) to model drought duration, severity and inter-arrival time jointly.

The use of copulas to quantify the joint behaviour of drought indices is gaining popularity too. Many drought indices derived by multivariate distributions have been proposed. For example the Multivariate Standardized Drought Index (MSDI) (Hao and Aghakouchak, 2013), which combines the SPI and the Standardized Soil Moisture Index (SSI), uses copula to form joint probabilities of precipitation and soil moisture content, while the Joint Drought Index (JDI) (Kao and Govindaraju, 2010) does the same for obtaining the joint probabilities while considering precipitation and streamflow. The composite Agrometeorological Drought Index accounting for Seasonality and Autocorrelation (AMDI-SA) combines two drought indices, the Modified SPI, and the Modified SSI, employing both the copula concept and the Kendall function (Bateni et al., 2018). The use of copulas seems promising and is highly effective when dealing with two or more variables. An advantage of copula functions is the fact that the index derived from this approach has a probabilistic form.

Both single and composite indices for agricultural drought monitoring showed some limitations, highlighted in Table 1 and Table 2. Single indices often rely on multiple inputs or are available only for some locations or identify all types of vegetation stresses. In any cases single indices do not account for the multivariate nature of drought. Composite indices often rely on relatively new datasets; in many cases a short period of record is available (for example the VegDri records start in 2009) or the index is not available in near-real time; some of them are specifically designed for a well identified region (the OBDI and the USDM are available only for the USA, the Combined Drought Indicator (CDI) only for Europe); other indices do not consider the meteorological aspect of drought (Temperature Vegetation Index, TVX, and Vegetation ~~Temeprature~~ Temperature Condition Index, VTCI, are based on the NDVI and the land surface temperature); other ones do not have a sufficiently refined spatial resolution (MSDI). Most of them, with the exception of AMDI-SA and MSDI are not expressed in probabilistic terms, therefore uncertainty quantification and evaluation is not an easy task.

In this paper, we propose:

1. A new drought index, the Probabilistic Precipitation Vegetation Index (PPVI), that takes the advantage of well consolidated indices, the Standardized Precipitation Index (SPI) (Mckee et al., 1993) and the Vegetation Health Index (VHI) (Kogan, 1997) and tries to overcome their individual limitations by coupling them in a probabilistic framework through the use of a bivariate normal distribution function.

90   2. A framework to identify a drought event using the new index, i.e. a set of rules for the definition of a drought event. When the set of conditions is verified, a drought event is identified based on the new index. Otherwise, no drought event is identified.

With respect to the indices already available in literature, we will show in this paper that the new index has some interesting features:

95   • it is able to identify drought-driven events of vegetation stress;

   • it is parsimonious in terms of number of inputs required;

   • it is a remote sensing product with high spatial and temporal resolution;

   • it is based on quasi-near real time datasets, with a relatively short latency time (less than one week);

   • more than 30 years of records are available at global scale for its calibration.

100   The paper is structured as follows: Sect.2 describes the datasets employed in the development of the new index and presents the methodology used to combine the SPI and the VHI; Sect. 3 illustrates the application to the case study, shows the validation process of the new index and compares the performance of the new index to those of the SPI and the VHI considered separately; in addition the advantages related to the adoption of the index and the possible applications in agricultural drought risk management are summarized.

105   ## 2   Datasets and Methods

2.1   Datasets

Two remote-sensing datasets were used: one for precipitation and the other for the VHI. Precipitation was retrieved from the satellite-only Climate Hazard Group Infrared Precipitation (CHIRP) dataset. CHIRP has a quasi-global coverage (50°S - 50°N), high spatial resolution (0,05 0.05°) and daily, pentadal and monthly temporal resolution. Records start from 1/1/1981.
110   CHIRP was chosen because it has been specifically developed to monitor agricultural drought. The use of CHIRP instead of CHIRPS (the Climate Hazard Group Infrared Precipitation with Stations) is related to the data latency time, which is shorter in the case of CHIRP since it doesn't include data from weather stations. Since the aim of the work is the development of an index for near-real time drought monitoring, the product with the shortest latency time was selected. CHIRPS data have a latency time of about three weeks (Funk et al., 2015), while CHIRP's latency is about 2 days, as can be checked on the dataset website (Climate Hazard Group, 2015). The development and the main characteristics of the dataset are described
115   in (Funk et al., 2015) Funk et al. (2015). In the present study CHIRP with a daily temporal resolution was used to have the possibility to compute weekly precipitation. Data are available on the project website (Climate Hazard Group, 1999).

The Vegetation Health Index was retrieved from the Global Vegetation Health Products (Global VHP) of the National Oceanic and Atmospheric Administration Center of Satellite Applications and Research (Kogan, 1997). Data can be retrieved

120 at the NOAA website (NOAA, 2011). The dataset contains Blended-VHP derived from VIIRS (2013-present) and AVHRR (1981-2012) GAC data. The dataset has 4km spatial resolution, weekly temporal resolution, and global coverage. Both the selected datasets are freely available.

2.2 Methods

2.2.1 The Standardized Precipitation Index

125 As previously mentioned, two consolidate drought indices were combined: the SPI and the VHI. The SPI was selected because it is a commonly used index to detect meteorological drought, it is standardized, therefore SPI values can be compared even in different climate regimes and it is recommended by the WMO (World Meteorological Organization, 2009).

SPI computation is based on a long-term precipitation record for a desired period. The precipitation record is then fitted to a probability distribution (in this work a gamma distribution was used), which is then transformed into a normal distribu-
130 tion. Traditionally monthly precipitation records are employed, and SPI is computed aggregating precipitation at a predefined timestep (for example 1 month, 3 months, 6 months, 9 months and 12 months are the aggregation periods suggested by the WMO (World Meteorological Organization, 2009)).

In the present work, weekly precipitation records were used. The SPI aggregation period was then selected and the index, computed over one of the the traditional aggregation periods, was updated every week. SPI is normal distributed by definition.
135 Conventionally drought starts when SPI is lower than -1 and ends when SPI comes back to the value of 0 (Mckee et al., 1993). Drought classification according to SPI, as proposed in (Mckee et al., 1993) Mckee et al. (1993) , is reported in Table 3. The percentages reported in the third column of Table 3 indicate the probability for SPI values to fall within the range reported in the second column of the same table.

2.2.2 The Vegetation Health Index

140 The VHI is a remote-sensing index developed to include the effects of temperature on vegetation; in fact, it combines the VCI with the Temperature Condition Index (TCI) (Kogan, 1995a), which is another remote-sensing index used to determine vegetation stress caused by temperature and excessive wetness. The VHI is based on a linear combination of VCI and TCI, $VHI = \alpha VCI + (1 - \alpha)TCI$. As suggested by Kogan et al. (2016) , when VCI and TCI contributions are not known $\alpha = 0.5$. One drawback of the VHI is the impossibility to identify the cause of the vegetation stress; in fact, vegetation can suffer because
145 of various events: excessive wetness, pests, fires, droughts or others. It is a biophysical indicator of a lack of precipitation but can also be seen as representing drought impacts on the ground (Bachmair et al., 2016). It goes from 0, which stands for vegetation in very bad conditions to 100, meaning perfectly healthy vegetation. The classification scheme of VHI, as proposed in (Dalezios et al., 2017) Dalezios et al. (2017) , is presented in Table 4.

The VHI is standardized to make comparisons with the SPI easier. As mentioned by Peters et al. (2002) , all remote-sensing
150 indices can be expressed as deviations from the mean; therefore, the standardized variable, VHI_{st}, is computed according to

the following equation:

$$VHI_{st} = \frac{VHI - \overline{VHI}}{\sigma} \tag{1}$$

where $\overline{VHI}$ is the mean of the distribution and σ its standard deviation. Thus, the same procedure proposed in Peters et al. (2002) in the case of the NDVI has been applied to the VHI. The standardized variable, VHI_{st}, has a distribution with 0 mean and 1 as
155   standard deviation.

2.2.3 The Probabilistic Precipitation Vegetation Index (PPVI)

The Probabilistic Precipitation Vegetation Index (PPVI) is a composite index that takes into account both meteorological drought through the SPI, and agricultural drought conditions by including the VHI.

In order to combine the two consolidated indices the following preparatory steps are performed:

160   1. Extraction of the area under study from both the datasets;

2. Regridding of both precipitation and the VHI to bring them to the same spatial resolution (0,05°);

3. Aggregation of precipitation at weekly timescale (CHIRP has daily temporal resolution);

4. Computation and weekly update of SPI according to the methodology proposed in ~~(USDA Risk Management Agency et al., 2006)~~ USDA Risk Management Agency et al. (2006) , where precipitation are fitted to a gamma distribution. The goodness of
165   fit to the gamma distribution has been verified by means of probability plot.

5. Standardization of the VHI, as previously described.

The combination of SPI and VHI is performed using a bivariate normal distribution function, as it is defined by ~~(Kotz et al., 2000)~~ Kotz et al. (2000) . The normality of the SPI and VHI_{st} distributions has been verified as will be shown in Sect. 3.2. Therefore it is acceptable to assume that the joint probability of the two considered distributions takes the form of the bivariate normal
170   for correlated variables:

$$f(s,v) = \frac{1}{2\pi\sigma_s\sigma_v\sqrt{1-\rho^2}} \exp\left(-\frac{1}{2(1-\rho^2)}\left[\frac{(s-\mu_s)^2}{\sigma_s} + \frac{(v-\mu_v)^2}{\sigma_v} + \frac{2\rho(s-\mu_s)(v-\mu_v)}{\sigma_s\sigma_v}\right]\right) \tag{2}$$

where the following notation is adopted: the *SPI* is identified as *s* and the VHI_{st} is identified as *v*. The mean and the standard deviation of the SPI distribution $f(s)$ are respectively, by construction, $\mu_s = 0$ and $\sigma_s = 1$ and the mean and standard deviation of the VHI_{st} distribution, $f(v)$ are respectively $\mu_v = 0$ and $\sigma_v = 1$. The covariance matrix Σ and the correlation coefficient ρ
175   are defined according to ~~Eq~~Eqs. 3 and ~~Eq.~~4 respectively, where σ_{sv} is the covariance between *s* and *v*.

$$\Sigma = \begin{bmatrix} \sigma_s^2 & \rho\sigma_s\sigma_v \\ \rho\sigma_s\sigma_v & \sigma_v^2 \end{bmatrix} \tag{3}$$

6

$$\rho = \frac{\sigma_{sv}}{\sigma_s \sigma_v} \tag{4}$$

To check the assumption of normality for the joint distribution, the joint probability values, retrieved from Eq.2 are plotted against the bivariate empirical cumulative distribution values (Fig.1), as done in (Kao and Govindaraju, 2010). The bivariate
180 empirical copula for the random variables *s* and *v* has been evaluated according to ~~(Nelsen, 2006)~~ Nelsen (2006) using the following equation:

$$C\left(\frac{i}{m}, \frac{j}{m}\right) = \frac{\#(s \le s_{(i)}, v \le v_{(j)})}{m} = \frac{m_1}{m} \tag{5}$$

where $s_{(i)}$ and $v_{(j)}$, $(1 \le i, j \le m)$ are ordered statistics of the *SPI* sample of size m, m_1 is the number of samples $(s_{(k)}, v_{(k)})$ satisfying $(s_{(k)} \le s_{(i)} \ and \ v_{(k)} \le v_{(j)})$ with $1 \le k \le m$. The resulting plot is shown in Fig.1.
185 Since the data lays on the 45°line it is fair to assume that the joint probability $f(s, v)$ is normal. Therefore, a normalization of the index is performed through normal quantile transformation.

By keeping the same probability intervals of the SPI, we can compute the PPVI values for the drought classification as it is shown in Table 5.

2.2.4 Identification of drought events

190 Once the index is defined the set of rules to establish when a grid cell is in drought should be identified. In particular, two parameters have to be identified:

1. A threshold *Z* of the index that marks the beginning of a drought in a grid cell.

2. A threshold *z* that marks the end of a drought in the same grid cell.

According to the model here proposed a drought in a grid cell starts when the index is lower than *Z* and ends when the index
195 is above to *z*. Then regional drought events are defined. Again, two parameters are identified: *N* and *n*. A drought events starts if more than *N* grid cells are in drought conditions and ends if less than *n* grid cells are in drought conditions.

2.2.5 Skill assessment

Observations of drought are compared with the model outputs for various combinations of thresholds *Z*, *z*, *N* and *n*. The Receiver Operating Characteristic (ROC) curve is used for this comparison. The ROC curve was at first used in signal detection; its
200 use in meteorological applications is documented and well described in ~~(Joliffe and Stephenson, 2012)~~ Joliffe and Stephenson (2012). The ROC curve is employed to classify instances, as in the present case. The ROC curve was already employed in various studies to compare the performance of a model versus observations with varying thresholds (Zhu et al., 2016; Khadr, 2016). The contingency matrix (shown in Table 6) is a two by two matrix to visualize the disposition of a set of instances. True positive or hits are represented by the weeks that are reported to be in drought conditions in the observations and are correctly

identified as drought weeks by the model. True negatives (correct rejections) are represented by those weeks that are not in drought according to both the observations and the model. Those weeks that are recorded as drought according to the observations but are not identified as drought weeks by the model, are considered as false negatives (missing events), while false positives (false alarms) are represented by the weeks that are not in drought conditions according to the observations but are identified as drought weeks by the model. In this paper for each combination of thresholds Z, z, N and n, Probability of Detection (POD), or hit rate, and Probability of False Detection (POFD), or false alarm rate, are computed according to ~~(Joliffe and Stephenson, 2012)~~ Joliffe and Stephenson (2012) with the following equations:

$$POD = \frac{TP}{TP + FN} \tag{6}$$

$$POFD = \frac{TN}{TN + FP} \tag{7}$$

where *TP*,*TN*,*FP* and *FN* are defined as in Table 6.

The optimal threshold for a ROC curve is the one for which the distance from the 45°degree line is maximum (Zhu et al., 2016). The performances of the model based on PPVI in identifying drought events have been evaluated on the case study described in the next section.

2.2.6 Case study

The case study region is Haiti. The country, which has an extension of 27.750 km^2 is located in the Caribbean's Great Antilles and shares the island of Hispaniola with the Dominican Republic. The climate is predominantly tropical, with daily temperatures ranging between 19°C and 28°C during winter and between 23°C and 33°C during summer. The island topography is varied; the central region is mainly mountainous, while the northern and western regions are near the coastline. Annual precipitation in the central region averages 1.200 mm, while in the lowlands it is about 550 mm (GFDRR, 2011). Haiti is subject to the variability associated with El Niño and La Niña phenomena, with El Niño bringing drier and hotter conditions and La Niña colder and wetter climate. Haiti experiences a first rainy season from April to July and a second, and most important, from August to the end of November. The dry season starts in December and goes on until the end of March (FEWSNET, 2019).

Haiti is divided administratively into 10 departments (Fig. 2), with people living mainly in the West, where the capital Port-au-Prince is located, and in the Artibonite. The total population in 2017 was about 11 million people (World Bank, 2017). Haiti is the poorest country in the Western Hemisphere, the economy is mainly agricultural. 67% of the country's area is devoted to agriculture, but only 4,35% of the agricultural area is irrigated (Trading Economics, 2013), posing a major threat to local production.

Haiti produces over half of the world's vetiver oil (used in cosmetics), and mangos and cocoa are the most important export crops. Two-fifths of all Haitians depend on the agriculture sector, mainly small-scale subsistence farming. The country is prone to all types of natural hazards. Earthquakes, storms, hurricanes, landslides, and droughts have caused huge damages and losses

in recent years. Haiti was ranked as the third most affected country by extreme weather events in terms of lives lost and economic damages in the period from 1994 to 2013 (GFDRR, 2011). More than 96% of the population lives in areas at risk of two or more hazards. The most frequent disasters are floods and storms but, when considering the number of affected people, droughts are the disasters involving the highest number of persons (Fig. 3).

240 Droughts threat the livelihoods of Haitians in many different ways. The scarcity of crops production means a rise in food prices, that brings to widespread food insecurity since the major part of people can't afford the increase. Unavailability of drinking water leads to cholera outbreaks among the population. Water is an issue also for breeders, who lose livestock on which they rely for milk production and meat consumption. In the period from 1980 to present more than 10 drought events have been reported by the government or the humanitarian organizations working in Haiti (Table 7). The worst drought was

245 the one of 2014-2017, affecting more than 3 million inhabitants (about one-third of Haiti's population).

Effective drought management is crucial for Haiti, but at present, a reliable early warning system for drought is still lacking. Weather stations on the ground are few and data records are often very short, therefore not useful for drought monitoring purposes on the entire country. Satellite images can be an effective and not expensive way to improve drought management and preparedness in the country.

250 # 3   Results and Discussion

3.1   Correlation analysis

Haiti has been divided into 987 grid cells, accounting for 90% of the country area. 1941 weeks were considered, starting from week 35 of 1981 and ending with week 52 of 2018. The release date of a new VHI image was considered as the starting date for a week. In the present study, four precipitation aggregation periods were considered (1 months, 2 months, 3 months and 6

255 months) and the corresponding values of SPI (SPI1, SPI2, SPI3 and SPI6) were computed in order to select the SPI aggregation timescale to be used to create the PPVI.

To evaluate the strength of the statistical relationship between the SPI at various timescales and the VHI a correlation analysis was then performed. Various studies have already evaluated the correlation among drought indices or between drought indices and exogenous variables; for example (Bonaccorso et al., 2015) investigated the correlation between SPI and ~~NAO, while~~

260 ~~(Hongshuo et al., 2014)~~ North Atlantic Oscillation (NAO), while Hongshuo et al. (2014) investigated the correlation between SPI (various aggregation periods) and the VHI. ~~While in the majority of the papers the~~ The Pearson correlation coefficient was employed ~~,~~ in the present study ~~the Spearman correlation coefficient was preferred~~ as a measure of the statistical relationship between the indices~~, as suggested in (Wedgbrow et al., 2002)~~. The number of significant correlations at 5% and 1% was evaluated for four SPI aggregation timescales (Table 8).

265 The highest number of significant correlations was found in the cases of SPI2 and SPI3, which exhibit very similar performances at 1% significant level. This finding is in agreement with previous studies such as ~~(Hongshuo et al., 2014) ,~~ Hongshuo et al. (2014) that found that VHI and SPI3 have the highest correlation for croplands, whereas VHI and 6-month SPI have the highest correlation for forest in the Southwest of China; and ~~(Ma'rufah et al., 2017)~~ Ma'rufah et al. (2017) that found

9

that significant correlation coefficient values on SPI3 and VHI are common in the southern part of Indonesia. Since SPI3 has been used in literature and the percentage of significant correlation at 1% level is relevant, it has been decided to aggregate SPI over a 3 months period and use SPI3 in the following discussion.

3.2 Normality of SPI and VHI distributions

Before computing PPVI as described in the previous sections, a test on the normality of the SPI3 and VHI_{st} distributions was performed. The goodness of fit of the SPI3 and the VHI_{st} distributions was verified through the histograms in Fig. 4 (panel (a) and (b) respectively), where the boxplots represent the relative frequencies of the SPI3 and VHI_{st} values. Both the SPI3 and the VHI_{st} data can therefore be considered normally distributed.

3.3 Selection of threshold values

PPVI was computed as described in Sect. 2.2 and its performance in identifying past drought events in Haiti when used in combination with the set of rules described in Sect. 2.2.4 was evaluated. To this end, the ROC curve classification methodology was applied. The set of rules implied that at first, cells in drought conditions were identified: drought started in a specific grid cell at week W when PPVI was lower than the threshold Z and ended when PPVI was up to the threshold z in the same grid cell at a week w (with w coming after W). Then a regional drought event was identified: the drought event started when more than N cells at a specific week W_1 were in drought conditions and ended at a week W_2 when few than n grid cells were in drought conditions. The comparison was performed on a weekly basis, with observations derived from the reported events described in Table 7.

The ROC curves were computed according to the following methodology: at first a combination of the thresholds Z, z, N and n was selected. On the basis of the set of rules established in Sect. 2.2.4, the ability of the selected combination of thresholds in reproducing the observations was assessed by computing *TP*, *TN*, *FP* and *FN* as defined in Table 6, together with POD and POFD. A couple (POFD, POD) represents a point in a ROC graph. Then one threshold among Z, z, N and n was selected. The selected threshold was variable during the analysis, while the other three were kept constant. The step of variation was identified according to the threshold maximum and minimum values. For each combination of the four thresholds (the varying one and the three fixed) *TP*, *TN*, *FP*, *FN* and POD and POFD were computed. The resulting set of couples (POFD, POD) represented the ROC curve for the considered set of thresholds.

The analysis was repeated by varying another threshold among Z, z, N and n. As an example, Fig. 5 shows four ROC curves for the thresholds in Table 9. Thresholds N and n in Table 9 are expressed as the percentage of the country's area instead as the number of grid cells. For each of the curves the best performing set of (Z, z, N and n) was selected by identifying the point farther from the 45°line, as done by ~~(Zhu et al., 2016)~~ Zhu et al. (2016) . The Area Under the Curve (AUC) was used as criteria to establish which of the ROC curves should be preferred (as was done by ~~(Dutra et al., 2014; Mason and Graham, 2002; Zhu et al., 2012)~~ Dutra et al. (2014); Mason and Graham (2002); Zhu et al. (2012)). An AUC near to 1 indicates good performance, while AUC of 0.5 indicates the model has no predictive skills. From Fig. 5 it is clear that the curve corresponding to the parameters defined as "Set 2" in Table 9 should be preferred, since the AUC is the closest to 1.

3.4 ~~Indices comparison~~Comparison of drought indices with observed drought events

The aim of this paragraph is not to validate in absolute terms the proposed methodology since the data record is too short to serve both for calibration and for validation. In the present section, instead, we provide a validation by comparing ~~PPVI with~~ the performance of PPVI in identifying observed drought events with the one of widely recognized and used indices such as SPI and VHI.

The performance of PPVI was then compared to the one of SPI3 and VHI considered separately. Thresholds analogous to Z and z were defined for SPI3 and VHI. Thresholds Z_S and z_S mark respectively the beginning and the end of drought conditions in a grid cell according to SPI3 and thresholds Z_V and z_V do the same in the case of VHI. Again the four thresholds Z, z, N, and n were varied in order to identify the optimal values. As an example Fig. 6 shows a comparison among the ROC curves for the three indices. In each panel of Fig. 6, n and z, z_S and z_V (for PPVI, SPI3 and VHI) remained constant, while Z, Z_S and Z_V were varying; N was fixed in each panel but varied among the panels. Z varied from -4 to -1.1 with a step equals to 0.1; Z_S varied from -3 to 0 with a step equals to 0.1 and Z_V varied from 10 to 40 with a step equal to 5.

It is clear from Fig. 6 that ~~PPVI identified the reported drought events better than SPI3 and VHI. AUC was 0,828 for PPVI, 0,740 for SPI3 and 0,784 for VHI~~the red curve, representing PPVI, is the furthest from the diagonal line in all the panels of the figure. The Area Under the Curve (AUC) was used as criteria to establish which index gave the best performances. AUC values are shown in Fig. 6 for each index and various configurations of the model. The AUC value of PPVI was in line with similar results reported in literature (Mwangi et al., 2014). As can be seen from Fig. 6, the new index provided better results with respect to the ones obtained with SPI3 or VHI considered separately. In all the four configurations shown in Fig. 6, the AUC for the curve constructed with PPVI was higher than the ones for SPI3 and VHI. The AUC values are in line with the ones considered good in the literature (see ~~(Khadr, 2016)~~ Khadr (2016)) for drought predictive skills. The optimal thresholds to configure the model when applied with each of the three considered indices were then determined by selecting the point farther from the 45°line, as done by ~~(Zhu et al., 2016)~~ Zhu et al. (2016) . The best configurations parameters are shown in Table 10~~and comes from the PPVI curve shown in panel (c) of Fig. 6.~~. The drought events were therefore identified using the optimal parameters (Table 10). A graphical representation of the performance of the model in reproducing observed drought events is given in Fig. 7. Only the period from 2000 to 2018 is shown.

The ability of the model in identifying the country area hit by the drought was also assessed. A visual comparison among the area under drought identified by the three indices was performed, as was done by ~~(Dutta et al., 2015)~~ Dutta et al. (2015) .

Here some significant weeks are shown. At first, week 45 of 1995 was considered. No drought events were reported in that period ~~. Figure 7~~ according to the information available in the analysed documents (see Table 7). Figure 8 shows that, while SPI3 identified all the southern part of the country as dry areas and VHI showed vegetation suffering in two departments (Centre and West), PPVI did not show signs of drought, except for a minor number of grid cells. Figure ~~8~~9 shows that in 2015, when the whole country was reported to be in severe drought conditions (see Table 7 and NOAA (2017); OXFAM and Action contre la Faim (2015)) PPVI captured well the pattern, only a few grid cells were not in drought conditions. The SPI3 was also able to catch the situation, while for the VHI only 58% of the county was in drought. During week 8 of 2012, only the Northern part of the country

11

was in drought (Fig. 9); five 10), as highlighted by USAID and FEWSNET (2012b) (see Table 7). Five departments were reported to be stressed (North, North West, North East, Artibonite, Centre, see Table 7). All the three indices showed the North West as the department most affected by drought when considering the percentage of the department area hit by the drought. PPVI then classified Artibonite, North, Centre and North East, while SPI3 as second and third most affected departments identified South and Grand Anse and VHI Centre and Nippes (Table 11).

Severity, duration and mean areal extent of the drought events identified by PPVI were computed. Severity was computed as the sum of all the values identified by the condition that a grid cell is in a drought condition when PPVI is lower than -1.8 and exits from drought when PPVI is up to -1.1. Duration is expressed in months and the mean areal extent is the average percentage of area in drought during a specific event. Results are presented in Table 12.

PPVI showed overall a better capacity in identifying drought events with respect to SPI3 and VHI considered separately. However, some false alarms still remain. This can be linked to the uncertainty in information on past drought events for the analysed area. Short-term droughts are often not reported in text-based documents, and information on drought start and end date were retrieved from documents that mainly described the impacts related to drought. PPVI showed a good agreement with reported information in identifying the areas of the country hit by the drought.

4 Conclusions

The timely identification of drought events is of great importance in agricultural areas, especially when rainfed agriculture is practiced. At the same time, the evaluation of the damages caused by drought is a key point to select appropriate risk management strategies, such as weather index insurance programs, agricultural index insurance, disaster financing and early action planning. The new composite index proposed in this paper, the Probabilistic Precipitation Vegetation Index, PPVI, is a powerful tool since it can identify events of vegetation stress, and at the same time, select among those the ones actually due to drought, thanks to the contemporary use of both VHI and SPI. As such it can be helpful in agricultural drought monitoring and can be used to identify drought events affecting a region, their severity and their duration as was shown in the case of Haiti. In particular, PPVI can be precious in those areas where rainfed agriculture is of vital importance since people rely on it for food production for personal consumption.

Among the interesting aspects of PPVI, there is the fact that few data are required for its computation: only precipitation and the VHI. This aspect is crucial, since many composite indicators able to identify agricultural droughts already exist, but large amounts of data are required to compute them. For example, the United States Drought Monitor combines more than 40-50 inputs, while other indices specific for agricultural drought monitoring, such as the VegDRI and the VegOut, require the use of temperature and oceanic indices. The number of parameters required to compute PPVI is lower even with respect to OBDI, SWS, CDI or CDSI.

A second most important advantage is that, since the SPI was computed starting from satellite precipitation (CHIRP dataset) and that the VHI is a remote-sensing drought index, PPVI is also a remote-sensing product. The use of datasets with global coverage means that PPVI is easily transferable and scalable over the entire globe. In addition, PPVI can be a very useful tool

in areas with scarce gauge coverage as the Caribbean Islands. Both precipitation and the VHI have a very high spatial and temporal resolution, thus allowing drought monitoring from satellite even in small areas. PPVI can be computed even in those regions with short data records, since the VHI has more than 30 years of records (data collection began in August 1981); and CHIRP precipitation are available from January 1981.

Both the SPI and the VHI are updated at weekly time-step since every week a new VHI image is released and the CHIRP precipitation dataset has a daily temporal resolution, therefore PPVI can be updated more frequently than other composite indices, such as CDI, which is updated every 10 days. In addition, due to the relatively short latency time (less than one week) of both the datasets employed to create PPVI, the index is available in near-real time, therefore allows the timely implementation of drought mitigation strategies. This last feature is of particular interest when PPVI is used to implement measure to reduce drought risk in agriculture, where a timely identification of drought is crucial to prevent damages to the sector.

Many advantages are also related to the adoption of the set of rules here proposed to identify drought events. First of all, these rules enable an objective and standardized identification of drought events from the mathematical point of view. Additionally, they can be adjusted according to the needs and the objectives of various possible end users of the model, such as farmers, governments or insurance companies.

The performances of PPVI in identifying drought events were tested in a specific case study (Haiti) and compared to the ones of SPI and VHI considered separately. PPVI performed better than the single indices considered separately in reproducing past drought events. PPVI identified drought areas in Haiti better than SPI and VHI even from the spatial point of view, thus it is more reliable than a single index. A comparison of PPVI performances with respect to the ones of other composite indices was not performed in the present study due to the unavailability of composite indices with the same characteristics of PPVI. In fact previous composite indices do not include both the meteorological and the agricultural aspect of drought or are not available globally, or cannot be computed with only remote sensing datasets.

Author contributions. This research is part of the PhD thesis from BM. BB and MM were both the thesis supervisors.

Competing interests. The authors declare that they have no conflict of interest.

References

Bachmair, S., Stahl, K., Collins, K., Hannaford, J., Acreman, M., Svoboda, M., Knutson, C., Smith, K. H., Wall, N., Fuchs, B., Crossman, N. D., and Overton, I. C.: Drought indicators revisited: the need for a wider consideration of environment and society, Wiley Interdisciplinary Reviews: Water, 3, 516–536, https://doi.org/10.1002/wat2.1154, http://doi.wiley.com/10.1002/wat2.1154, 2016.

Barnett, B. J. and Mahul, O.: Weather Index Insurance for Agriculture and Rural Areas in Lower-Income Countries, American Journal of Agricultural Economics, 89, 1241–1247, 2007.

Bateni, M., Behmanesh, J., and Bazrafshan, J.: Composite Agrometeorological Drought Index Accounting for Seasonality and Autocorrelation, Journal of Hydrologic Engineering, 23, https://doi.org/10.1061/(ASCE)HE.1943-5584.0001654, 2018.

BC Ministry for Agriculture: Soil water storage capacity and available soil moisture, Tech. rep., 2015.

Bergman, K., Sabol, P., and Miskus, D.: Experimental Indices for monitoring global drought conditions, Proceedings of 13th Annual Climate Diagnostics Workshop,, 1988.

Bijaber, N., Hadani, D. E., Saidi, M., Svoboda, M. D., Wardlow, B. D., Hain, C. R., Poulsen, C. C., Yessef, M., and Rochdi, A.: Developing a Remotely Sensed Drought Monitoring Indicator for Morocco, Geosciences, 8, 1–18, https://doi.org/10.3390/geosciences8020055, 2018.

Bonaccorso, B., Cancelliere, A., and Rossi, G.: Methods for Drought Analysis and Forecasting, in: Handbook of Methods and Applications of Statistics in the Atmospheric and Earth Sciences, pp. 150–184, 2012.

Bonaccorso, B., Cancelliere, A., and Rossi, G.: Probabilistic forecasting of drought class transitions in Sicily (Italy) using Standardized Precipitation Index and North Atlantic Oscillation Index, Journal of Hydrology, 526, 136–150, https://doi.org/10.1016/j.jhydrol.2015.01.070, http://dx.doi.org/10.1016/j.jhydrol.2015.01.070, 2015.

Brown, J. F., Wardlow, B. D., Tadesse, T., and Hayes, M. J.: The Vegetation Drought Response Index (VegDRI): A New Integrated Approach for Monitoring Drought Stress in Vegetation, GIScience & Remote Sensing, 45, https://doi.org/10.2747/1548-1603.45.1.16, 2008.

CIAT: Atlas des menaces naturelles en Haiti, Tech. rep., http://ciat.gouv.ht/articles/atlas-des-menaces-naturelles-en-haiti, 2017.

Climate Hazard Group: Climate Hazard Group InfraRed Precipitation data archive, ftp://ftp.chg.ucsb.edu/pub/org/chg/products/CHIRP/, 1999.

Climate Hazard Group: Chirp daily, ftp://ftp.chg.ucsb.edu/pub/org/chg/products/CHIRP/daily/, 2015.

CNSA/MARNDR and FEWSNET: Haiti Food Security Update September 2009, https://reliefweb.int/report/haiti/haiti-food-security-update-april-september-2009, 2009.

CRED: EM-DAT The International Disaster Database, http://emdat.be/emdat{_}db/, 2017.

Dalezios, N. R., Tarquis, A. M., and Eslamian, S.: Droughts, in: Environmental Hazards Methodologies for Risk Assessment and Management, edited by Dalezios, N. R., chap. 5, IWA Publishing, https://doi.org/10.2166/9781780407135, 2017.

Dieker, E., van Lanen, H. A. J., and Svoboda, M.: Comparison of three drought monitoring tools in the USA, Tech. Rep. 25, 2010.

Drechsler, M. and Soe, W.: Early Warning , Early Action The Use of Predictive Tools in Drought Response through Ethiopia ' s Productive Safety Net Programme, Tech. Rep. June, World Bank, 2016.

Dutra, E., Pozzi, W., Wetterhall, F., Giuseppe, F. D., Magnusson, L., Naumann, G., Barbosa, P., and Vogt, J.: Global meteorological drought – Part 2 : Seasonal forecasts, Hydrology and Earth System Sciences, 18, 2669–2678, https://doi.org/10.5194/hess-18-2669-2014, 2014.

Dutta, D., Kundu, A., Patel, N., Saha, S., and Iddiqui, A.: Assessment of agricultural drought in Rajasthan (India) using remote sensing derived Vegetation Condition Index (VCI) and Standardized Precipitation Index (SPI), The Egyptian Journal of Remote Sensing and Space Sciences, 18, 53–63, https://doi.org/10.1016/j.ejrs.2015.03.006, 2015.

14

FEWSNET: HAITI Food Security Outlook Update May 2013, Tech. Rep. May, https://reliefweb.int/report/haiti/haiti-food-security-outlook-update-may-2013, 2013.

FEWSNET: Haiti seasonal calendar, http://fews.net/central-america-and-caribbean/haiti, 2019.

Funk, C., Peterson, P., Landsfeld, M., Pedreros, D., Verdin, J., Shukla, S., Husak, G., Rowland, J., Harrison, L., Hoell, A., and Michaelsen, J.: The climate hazards infrared precipitation with stations - A new environmental record for monitoring extremes, Scientific Data, 2, 1–21, https://doi.org/10.1038/sdata.2015.66, 2015.

GFDRR: Climate Risk and Adaptation Country Profile: vulnerability, risk reduction and adaptation to climate change in Haiti, Tech. Rep. April, 2011.

Gu, Y., Hunt, E., Wardlow, B., Basara, J. B., Brown, J. F., and Verdin, J. P.: Evaluation of MODIS NDVI and NDWI for vegetation drought monitoring using Oklahoma Mesonet soil moisture data, Geophysical Research Letters, 35, 1–5, https://doi.org/10.1029/2008GL035772, 2008.

Guimarães Nobre, G., Davenport, F., Bischiniotis, K., Veldkamp, T., Jongman, B., Funk, C. C., Husak, G., Ward, P. J., and Aerts, J. C. J. H.: Financing agricultural drought risk through ex-ante cash transfers, Science of the Total Environment, 653, 523–535, https://doi.org/10.1016/j.scitotenv.2018.10.406, https://doi.org/10.1016/j.scitotenv.2018.10.406, 2019.

Hao, Z. and Aghakouchak, A.: Advanc es in Water Resou rces Multivariate Standardized Drought Index : A parametric multi-index model, Advances in Water Resources, 57, 12–18, https://doi.org/10.1016/j.advwatres.2013.03.009, http://dx.doi.org/10.1016/j.advwatres.2013.03.009, 2013.

Hao, Z. and Singh, V.: Review of dependence modeling in hydrology and water resources, Progress in Physical Geography, 40, 549–578, https://doi.org/10.1177/0309133316632460, 2016.

Hao, Z. and Singh, V. P.: Drought characterization from a multivariate perspective : A review, Journal of Hydrology, 527, 668–678, https://doi.org/10.1016/j.jhydrol.2015.05.031, http://dx.doi.org/10.1016/j.jhydrol.2015.05.031, 2015.

Hongshuo, W., Hui, L., and Desheng, L.: Remotely sensed drought index and its responses to meteorological drought in Southwest China, Remote Sensing Letters, 5, 2014.

Idso, S., Jackson, R., Pinter, P. J., Reginato, R., and Hatfield, J.: Normalizing the stress-degree-day parameter for environmental variability, Agricultural Meteorology, 24, 1981.

Jensen, N. and Barrett, C.: Agricultural Index Insurance for Development, Applied Economic Perspectives and Policy, 39, 199–219, https://doi.org/10.1093/aepp/ppw022, 2017.

Joliffe, I. T. and Stephenson, D. B.: Forecast Verification: a practitioner's guide in Atmospheric Science, https://doi.org/10.1016/B978-0-12-385022-5.00008-7, 2012.

Kao, S.-c. and Govindaraju, R. S.: A copula-based joint deficit index for droughts, Journal of Hydrology, 380, 121–134, https://doi.org/10.1016/j.jhydrol.2009.10.029, http://dx.doi.org/10.1016/j.jhydrol.2009.10.029, 2010.

Karamouz, M., Rasouli, K., and Nazif, S.: Development of a Hybrid Index for Drought Prediction : Case Study, Journal of Hydrologic Engineering, 14, 617–627, 2009.

Keyantash, J. and Dracup, J.: An aggregate drought index: Assessing drought severity based on fluctuations in the hydrologic cycle and surface water storage, Water Resources Research, 40, 2004.

Khadr, M.: Forecasting of meteorological drought using Hidden Markov Model (case study : The upper Blue Nile river basin , Ethiopia), Ain Shams Engineering Journal, 7, 47–56, https://doi.org/10.1016/j.asej.2015.11.005, http://dx.doi.org/10.1016/j.asej.2015.11.005, 2016.

Kogan, F. N.: Remote sensing of weather impacts on vegetation in non-homogeneous areas, International Journal of Remote Sensing, 11, 1405–1419, 1990.

Kogan, F. N.: Droughts of the late 1980s in the United States as derived from NOAA polarorbiting satellite data, Bulletin of the American Meteorology Society, 76, 655–668, 1995a.

470 Kogan, F. N.: Application of vegetation index and brightness temperature for drought detection, Advances in Space Research, 15, 2761–2782, 1995b.

Kogan, F. N.: Global Drought Watch from Space, Bulletin of the American Meteorological Society, 78, 621–636, 1997.

Kogan, F. N., Guo, W., Strashnaia, A., A., K., Chub, O., and Virchenko, O.: Modelling and prediction of crop losses from NOAA polar-orbiting operational satellites, Geomatics, Natural Hazards and Risk, 7, 886–900, https://doi.org/10.1080/19475705.2015.1009178, 2016.

475 Kotz, S., Balakrishnan, N., and Johnson, N. L.: Continuous Multivariate Distributions, John Wiley & Sons, second edi edn., https://doi.org/10.1002/0471722065, 2000.

Lambin, E. and Ehrlich, D.: Combining vegetation indices and surface temperature for land-cover mapping at broad spatial scales, International Journal of Remote Sensing, 16, 1995.

Linnerooth-Bayer, J. and Hochrainer-Stigler, S.: Financial instruments for disaster risk management and climate change adaptation, Climatic 480 Change, 133, 2015.

Liu, W. and Kogan, F. N.: Monitoring regional drought using the Vegetation Condition Index, International Journal of Remote Sensing, 17, 2761–2782, 1996.

Ma'rufah, U., Hidayat, R., and Prasati, I.: Analysis of relationship between meteorological and agricultural drought using standardized precipitation index and vegetation health index, in: Earth and Environmental Science, vol. 54, p. 7, https://doi.org/10.1088/1742-485 6596/755/1/011001, 2017.

Mason, S. and Graham, N.: Area beneath the relative operating characteristics (ROC) and relative operating levels (ROL) curves: statistical significance and interpretation, Quarterly Journal of the Royal Meteorological Society, 128, 2145–2166, https://doi.org/10.1016/B978-1-4377-0795-3.00025-9, 2002.

Matera, A., Fontana, G., and Marletto, V.: Use Of a New Agricultural Drought Index Within a Regional Drought Observatory, in: Methods 490 and Tools for Drought Analysis and Management, edited by Rossi, G., pp. 103–124, Springer, 2007.

Mckee, T. B., Doesken, N. J., and Kleist, J.: The relationship of drought frequency and duration to time scales, in: AMS 8th Conference on Applied Climatology, January, pp. 179–184, https://doi.org/10490403, http://ccc.atmos.colostate.edu/relationshipofdroughtfrequency.pdf, 1993.

Meyer, S. J., Hubbard, K. G., and Wilhite, D. A.: Crop-Specific Drought Index for Corn: I. Model Development and Validation, Agronomy 495 Journal, 86, 388–395, https://doi.org/10.2134/agronj1993.00021962008500020040x, 1993.

Mora-Castro, S.: Personal communication.

Mora-Castro, S.: Etude de reconaissance sur les differents types des menaces naturelles dans le basin versant de l'Artibonite, Haiti, Tech. rep., Ingeosa, Port au Prince, 1986.

Mwangi, E., Wetterhall, F., Dutra, E., Di Giuseppe, F., and Pappenberger, F.: Forecasting droughts in East Africa, Hydrology and Earth 500 System Sciences, 18, 611–620, https://doi.org/10.5194/hess-18-611-2014, 2014.

Narasimhan, B. and Srinivasan, R.: Development and evaluation of Soil Moisture Deficit Index (SMDI) and Evapotran-spiration Deficit Index (ETDI) for agricultural drought monitoring, Agricultural and Forest Meteorology, 133, 69–88, https://doi.org/10.1016/j.agrformet.2005.07.012, 2005.

Nelsen, R. B.: An Introduction to Copulas, Springer-Verlag, New York, 2 edn., https://doi.org/10.1007/0-387-28678-0, 2006.

505 NOAA: STAR—Global Vegetation Health Products. National Oceanic and Atmospheric Administration (NOAA), https://www.star.nesdis.noaa.gov/smcd/emb/vci/VH/vh{_}ftp.php, 2011.

NOAA: Climate Prediction Center ' s Hispaniola Hazards Outlook: October 5- October 11, 2017, Tech. rep., NOAA, 2017.

NOAA, USAID, and FEWSNET: Climate Prediction Center ' s Hispaniola Hazards Outlook For USAID / FEWS-NET Jult 11-July 17, 2013, Tech. rep., 2013.

510 OXFAM and Action contre la Faim: Etat des lieux de la situation de secheresse Dans les departements du Nord Ouest et du Haut Artibonite, Tech. rep., https://reliefweb.int/report/haiti/tat-des-lieux-de-la-situation-de-s-cheresse-dans-le-d-partement-du-nord-ouest-et-dans, 2015.

Palmer, W. C.: Keeping Track of Crop Moisture Conditions, Nationwide: The New Crop Moisture Index, Weatherwise, 21, 156–161, https://doi.org/10.1080/00431672.1968.9932814, 1968.

515 Peters, A. J., Walter-Shea, E. A., Ji, L., Vina, A., Hayes, M., and Svoboda, M. D.: Drought monitoring with NDVI-based Standardized Vegetation Index, Photogrammetric enginnering and remote sensing, 68, 71–75, 2002.

Sepulcre-Canto, G., Horion, S., Singleton, A., Carrao, H., and Vogt, J.: Development of a Combined Drought Indicator to detect agricultural drought in Europe, Natural Hazards and Earth System Sciences, 12, 3519–3531, https://doi.org/10.5194/nhess-12-3519-2012, 2012.

Serinaldi, F., Bonaccorso, B., Cancelliere, A., and Grimaldi, S.: Probabilistic characterization of drought properties through copulas, Physics

520 and Chemistry of the Earth, 34, 596–605, https://doi.org/10.1016/j.pce.2008.09.004, http://dx.doi.org/10.1016/j.pce.2008.09.004, 2009.

Sheffield, J. and Wood, E. F.: Drought: past problems and future scenarios, Routledge, 2011.

Shiau, J.-T.: Fitting Drought Duration and Severity with Two-Dimensional Copulas, Water Resources Management, 20, 795–815, https://doi.org/10.1007/s11269-005-9008-9, 2006.

Shiau, J.-T., Feng, S., and Nadarajah, S.: Assessment of hydrological droughts for the Yellow River, China, using copulas, Hydrological

525 Processes, 21, 2157–2163, 2007.

Songbai, S. and Singh, V. P.: Frequency analysis of droughts using the Plackett copula and parameter estimation by genetic algorithm, Stochastic Environmental Research and Risk Assessment, 24, 783–805, 2010.

Svoboda, M., Lecomte, D., Hayes, M., Heim, R., Gleason, K., Angel, J., Rippey, B., Tinker, R., Palecki, M., Stooksbury, D., Miskus, D., and Stephens, S.: The drought monitor, Bulletin of the American Meteorological Society, 83, 1181–1190, 2002.

530 Tadesse, T. and Wardlow, B. D.: The Vegetation Outlook (VegOut): A New Tool for Providing Outlooks of General Vegetation Conditions Using Data Mining Techniques, in: 7th IEEE International Conference on Data Mining Workshop, January, pp. 667–672, 2007.

Thornthwaite, C. and Mather, J.: The water balance, Climatology, 8, 1955.

Trading Economics: Haiti - Agricultural irrigated land (Percentage of total agricultural land), https://tradingeconomics.com/haiti/agricultural-irrigated-land-percent-of-total-agricultural-land-wb-data.html, 2013.

535 USAID and FEWSNET: HAITI Food Security Outlook Update June 2012, Tech. Rep. April, https://reliefweb.int/report/haiti/haiti-food-security-outlook-update-june-2012, 2012a.

USAID and FEWSNET: HAITI : Food Security Outlook Update March 2012, Tech. Rep. February, FEWSNET, http://fews.net/sites/default/files/documents/reports/Haiti{_}FSOU{_}2012{_}03{_}En{_}Final.pdf, 2012b.

USAID, MARNDR/CNSA, and FEWSNET: HAITI : Food Security Outlook Update June 2011, Tech. Rep. June, https://reliefweb.int/report/

540 haiti/food-security-outlook-update-june-2011, 2011.

USDA Risk Management Agency, National Drought Mitigation Center, and University of Nebraska Lincoln: Weekly SPI, http://greenleaf.unl.edu/, 2006.

Wang, L. and Qu, J. J.: NMDI : A normalized multi-band drought index for monitoring soil and vegetation moisture with satellite remote sensing, Geophysical Research Letters, 34, 1–5, https://doi.org/10.1029/2007GL031021, 2007.

545 Wang, L., Li, X., Gong, J., and Song, C.: Vegetation temperature condition index and its application for drought monitoring, in: Geoscience and Remote Sensing Symposium, pp. 141–143, 2001.

Wedgbrow, C. S., Wilby, R. L., and Fox, H. R.: Prospects for seasnal forecasting of summer drought and low river flow anomalies in England and Wales, International Journal of Climatology, 22, 219–236, https://doi.org/10.1002/joc.735, 2002.

Wilhite, D. A.: Drought as a natural hazard: Concepts and definitions, in: Drought: A Global Assessment, edited by Wilhite, D. A., chap. 1,
550 pp. 3–18, Routledge, London, 2000.

World Bank: Haiti data, https://data.worldbank.org/country/haiti, 2017.

World Meteorological Organization: Standardized Precipitation Index User Guide, Tech. Rep. 1090, 2009.

World Meteorological Organization and Global Water Partnership: Handbook of Drought Indicators and Indices, 1173, https://doi.org/10.1201/9781315265551-12, www.droughtmanagement.info, 2016.

555 Zargar, A., Sadiq, R., Naser, B., and Khan, F. I.: A review of drought indices, Environmental Reviews, 19, 333–349, https://doi.org/10.1139/a11-013, 2011.

Zhu, J., Pollanen, M., Abdella, K., and Cater, B.: Modeling Drought Option Contracts, ISRN Applied Mathematics, 2012, 1–16, https://doi.org/10.5402/2012/251835, http://www.hindawi.com/isrn/appmath/2012/251835/, 2012.

Zhu, Y., Wang, W., Singh, V. P., and Liu, Y.: Combined use of meteorological drought indices at multi-time scales for improving hydrological
560 drought detection, Science of the Total Environment, 571, 1058–1068, https://doi.org/10.1016/j.scitotenv.2016.07.096, http://dx.doi.org/10.1016/j.scitotenv.2016.07.096, 2016.
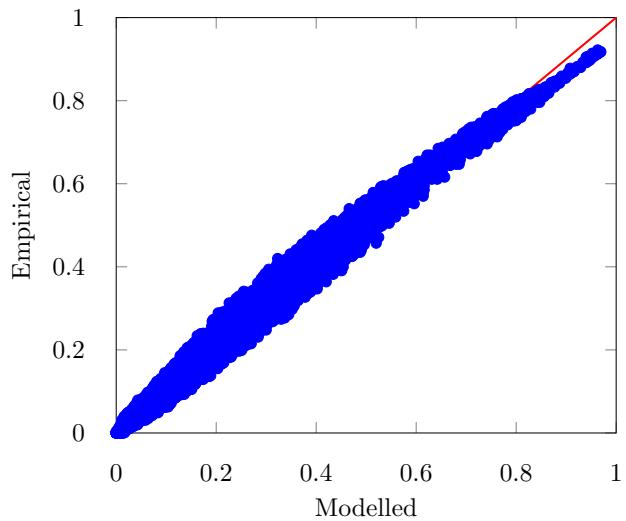
Figure 1. PPVI validation: empirical copula versus bivariate joint probability function. The red line corresponds to the 45°line. Joint probability values have been computed from Eq. 2, while empirical copula values according to Eq. 5.

Figure 2. Map of Haiti departments.
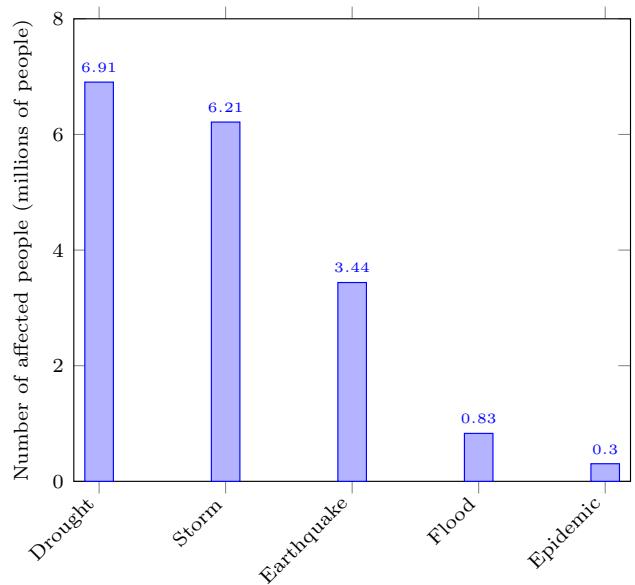
**Figure 3.** Number of people affected by natural disasters in Haiti (1900-2018). Source (CRED, 2017).
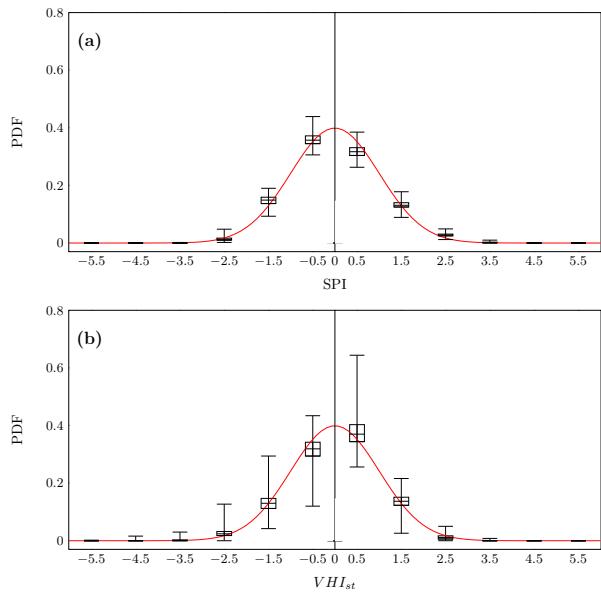
Figure 4. 4(a): distribution of SPI values; 4(b):distribution of VHI_{st} values. The red line represents the pdf of the standard normal distribution; boxplots represent the percentage of values lying in the range; 12 ranges were considered; starting from -6 and ending with 6 with a step equal to 1.
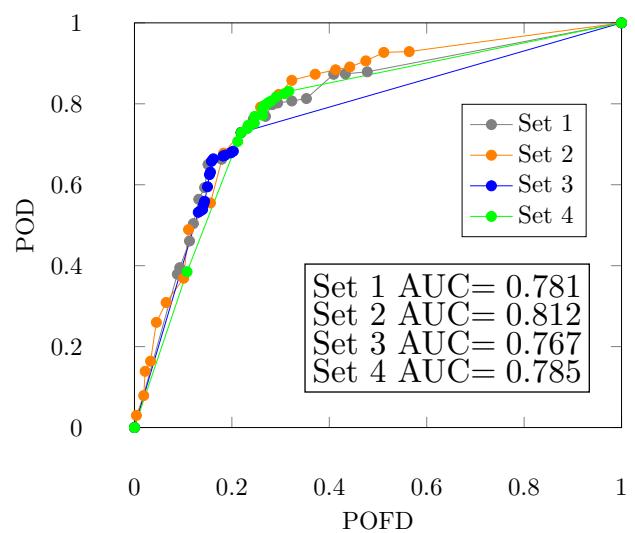
Figure 5. ROC curves for the set of thresholds reported in Table 9.
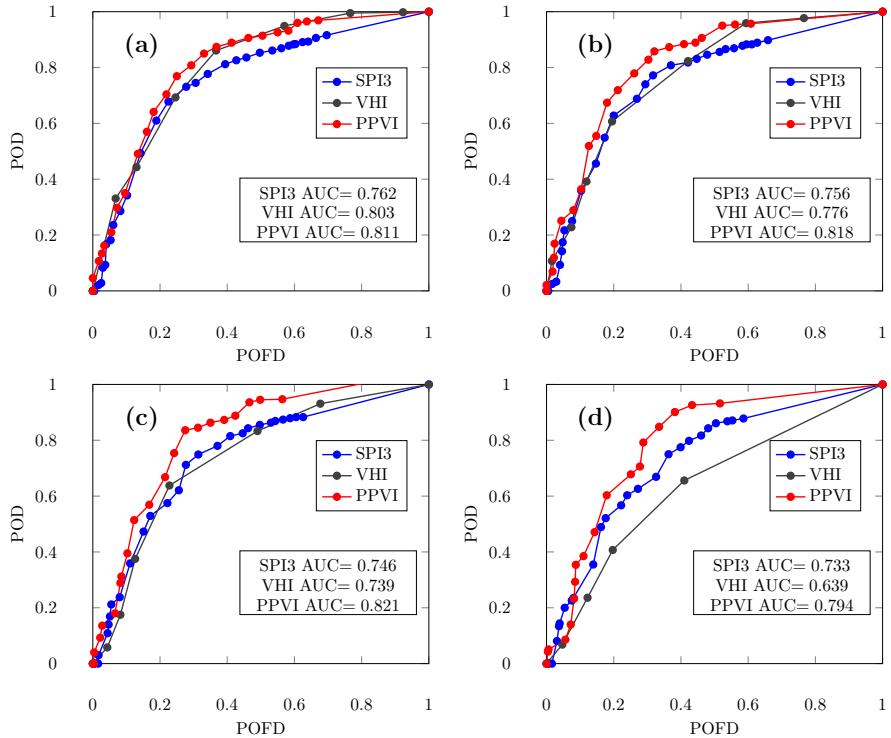
Figure 6. Comparison among the performances of SPI3, VHI and PPVI in identifying reported drought events; thresholds Z, Z_S and Z_V are varying, $z = -1.1$, $z_S = 0$ and $z_V = 40$; $n = 80$ and four cases for N are shown: (a): $N = 10\%$, (b): $N = 20\%$; (c):$N = 30\%$ and (d): $N = 50\%$.
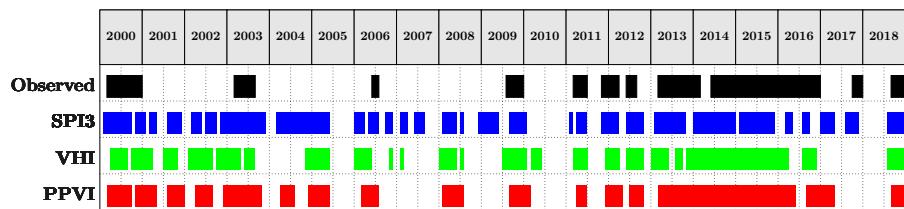
Figure 7. Comparison between observed drought events and drought events identified by PPVI, SPI3 and VHI when calibrated with the best performing parameters shown in Table 10. The comparison is shown for the period from 2000 to 2018
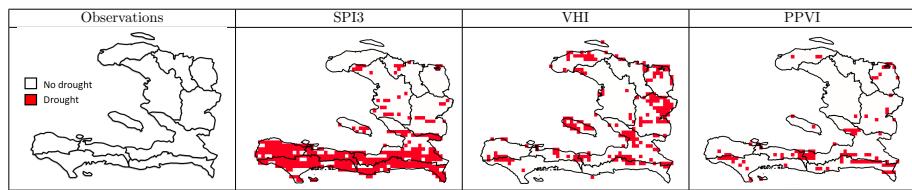
Figure 8. Comparison of the performance of SPI3, VHI, and PPVI in identifying the areas hit by drought. Week 45 of 1995. Departments highlighted in red are the ones in drought according to observations (Table 7), ~~black~~ red cells are the ones in drought condition according to the various indices.
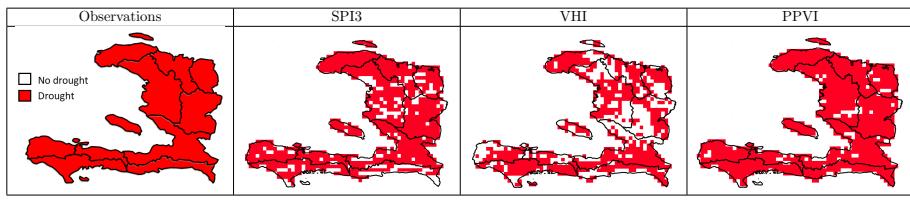
Figure 9. Same as Fig. ~~7~~ 8 but for week 33 of 2015. Departments highlighted in red are the ones in drought according to observations, ~~black~~ red cells are the ones in drought condition according to the various indices.
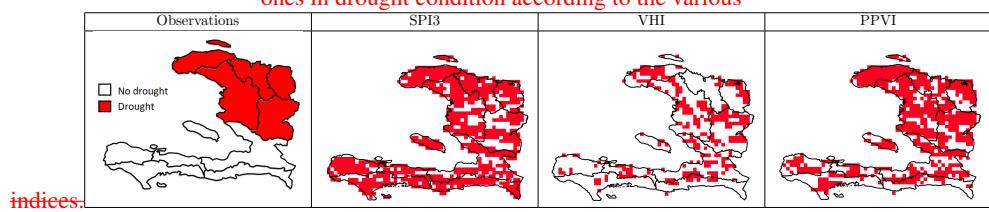
Figure 10. Same as Fig. 8 but for week 8 of 2012. Departments highlighted in red are the ones in drought according to observations, red cells are the ones in drought condition according to the various indices.

Table 1. An overview of indices used in agricultural drought monitoring; Met=Meteorological, Hydro=Hydrological, Ag=Agricultural.

| Index	Inputs	Drought type	Pros	Cons	Reference
ETDI	Modeled (SWAT)	Ag	Analysis of both actual and potential ET	Complex calculations	(Narasimhan and Srinivasan, 2005)
NDVI	Near-infrared	Ag	High resolution, global coverage, remote-sensing	Need for data processing	(Kogan, 1995a)
SMAI	Precipitation, Temperature, Available water content	Ag	Water balance approach	Data requirements	(Bergman et al., 1988)
SMDI	Modeled (SWAT)	Ag	Adaptable to different crop types	Based upon output from SWAT	(Narasimhan and Srinivasan, 2005)
SSI	Soil moisture	Ag	Uses soil moisture only, standardized	Based on one variable	(Hao and Aghakouchak, 2013)
SVI	VCI	Ag	Standardized, remote-sensing	Scarcerly employed	(Peters et al., 2002)
SWS	Available Water content, Rooting depth, Soil water deficit, Soil type	Ag	Well known calculations	Poor performance on non-homogeneous soils	(BC Ministry for Agriculture, 2015)
TCI	Brightness temperature	Ag	High resolution, global coverage, remote-sensing	Only brightness temperature is considered	(Kogan, 1995a)
VCI	NDVI	Ag	High resolution, global coverage, remote-sensing	Identifies all vegetation stresses, not only the ones due to drought	(Liu and Kogan, 1996)
CMI	Precipitation, Temperature	Ag	Weekly temporal resolution	Specifically developed for grain-producing regions in the USA	(Palmer, 1968)

29

Table 1. Continued.

Index	Inputs	Drought type	Pros	Cons	Reference
CSDI	Precipitation, Temperature, wind speed, solar radiation, dewpoint temperature, soil profile, plant phenology	Ag	Very specific for each crop, based on plant development	Many inputs with a daily temporal resolution	(Meyer et al., 1993)
CWSI	Actual and potential evapotranspiration	Ag	Useful for irrigation scheduling, remote-sensing	To be computed from MODIS data	(Idso et al., 1981)
NMDI	NDVI	Ag	Uses vegetation condition and soil water content	Poor performance in areas with sparse vegetation	(Wang and Qu, 2007)
RSM	Precipitation, Temperature, Evapotranspiration, Soil properties, Crop features, Crop management practice	Ag	Computes the water balance with various methods	Need for multiple inputs	(Thornthwaite and Mather, 1955)
DTx	Modeled (water balance)	Ag	Computes an integrated transpiration deficit over a period of time	Need for multiple inputs	(Matera et al., 2007)
ADI	Precipitation, Snow water content, Streamflow, Reservoir storage, Evapotranspiration, Soil water content	Met Hydro Ag	Water balance approach	Need for multiple inputs	(Keyantash and Dracup, 2004)

Table 2. An overview of aggregate and composite drought indices useful for agricultural drought monitoring; Met=Meteorological, Hydro=Hydrological, Ag=Agricultural.

Index	Inputs	Drought type	Pros	Cons	Reference
VegDRI	SPI, NDVI, PDSI	Ag	Use of surface and remote-sensing data	Short period of record, Available only for the contiguous USA	(Brown et al., 2008)
VHI	VCI, TCI	Ag	High temporal resolution, global coverage at a high spatial resolution, 30+ years of records	Identifies all types of vegetation stress, not only the drought-related ones	(Kogan, 1990)
MSDI	SPI, SSI	Met Ag	Global coverage, remote-sensing	Grid size may not represent all areas and climate regimes equally well; short period of records	(Hao and Aghakouchak, 2013)
CDI	SPI3, fAPAR, SMA	Met Ag	10-day temporal resolution, high spatial resolution (5km)	Short period of record (2012), Available only in Europe, hard to replicate	(Sepulcre-Canto et al., 2012)
Morocco CDI	SPI, ET, LST, NDVI	Met Ag	High spatial resolution (5km)	Monthly temporal resolution; available for Morocco only, short period of record	(Bijaber et al., 2018)

31

Table 2. Continued.

Index	Inputs	Drought type	Pros	Cons	Reference
Hybrid DI	SPI, SWSI, PDSI	Met Hydro Ag	Function of damage, includes all types of droughts	Need for detailed information on economic damages	(Karamouz et al., 2009)
VegOut	SPI, NDVI, oceanic indices	Met Ag	Combination of climate information, vegetation condition, oceanic indices, and land cover	Need for a high number of parameters	(Tadesse and Wardlow, 2007)
OBDI	Precipitation, MPDI, Soil moisture	Met Ag	First attempt to combine and weight various inputs	Specifically designed for the USA	(Dieker et al., 2010)
USDM	PDSI, Soil moisture, Streamflow, Percent of normal precipitation, SPI, OBDI	Met Hydro Ag	Combines many inputs and expert knowledge, weekly temporal resolution	Available only for the USA	(Svoboda et al., 2002)
TVX	NDVI, LST	Ag	Combination of NDVI and temperature effects, remote-sensing	To be computed from NDVI and LST datasets	(Lambin and Ehrlich, 1995)
VTCI	NDVI, LST	Ag	Combination of NDVI and temperature effects, remote-sensing	To be computed from NDVI and LST datasets	(Wang et al., 2001)
AMDI-SA	MSPI, MSSI	Met Ag	Combination of SPI and SSI; standardized	Complex calculations	(Bateni et al., 2018)

32

Table 3. Drought classification based on SPI according to (Mckee et al., 1993).

Category	SPI	Probability (%)
Extremely wet	2.00 and above	2.3
Severely wet	1.50 to 1.99	4.4
Moderately wet	1.00 to 1.49	9.2
Near normal	-0.99 to 0.99	68.2
Moderately dry	-1.49 to -1.00	9.2
Severely dry	-1.50 to -1.99	4.4
Extremely dry	-2 and below	2.3

Table 4. Drought classification based on VHI according to (Dalezios et al., 2017).

Category	VHI
Extremely dry	≤ 10
Severely dry	≤ 20
Moderately dry	≤ 30
Mild dry	≤ 40
Normal	> 40

Table 5. Drought classification according to PPVI.

Category	PPVI	Probability (%)
Extremely wet	1.04 and above	2.3
Severely wet	0.58 to 1.03	4.4
Moderately wet	0.13 to 0.57	9.2
Near normal	-1.68 to 0.12	68.2
Moderately dry	-2.14 to -1.69	9.2
Severely dry	-2.15 to -2.59	4.4
Extremely dry	-2.6 and below	2.3

Table 6. Contingency table for the deterministic estimates of a series of binary events (Joliffe and Stephenson, 2012).

Events estimated	Events Observed		
	Yes	No	Total
Yes	TP (True Positive or Hits)	FP (False Positive or False Alarms)	$TP + FP$
No	FN (False Negative or Missing)	TN (True Negative or Corret rejections)	$FN + TN$
Total	$TP + FN$	$FP + TN$	$TP + FP + FN + TN = T$

Table 7. Reported drought events in Haiti from 1980 to present.

Year	Department	Affected people	% population	Source
1981	South, Grand Anse, West	103'000	2	(Mora-Castro, 1986; CIAT, 2017)
1982-1983	South, South East, North West, North East	333'000	5.75	(Mora-Castro)
1984-1985	North West	13'500	2	(Mora-Castro, 1986; CIAT, 2017)
1986	All country			(Mora-Castro)
1990-1992	All country	1'000'000	14	(Mora-Castro)
1997	North West, North, North East	50'000	0.64	(CIAT, 2017)
2000	All ~~country~~ country			(Mora-Castro)
2003	North West	35'000	0.41	(CIAT, 2017)
End 2009	North West			(CNSA/MARNDR and FEWSNET, 2009)
2011-2012	North, North West, North East, Artibonite, Centre			(USAID et al., 2011; USAID and FEWSNET, 2012a)
2013	All country	> 143'000	1.5	(NOAA et al., 2013; FEWSNET, 2013)
2014-2017	All country	3'600'000	33	(OXFAM and Action contre la Faim, 2015; NOAA, 2017)

Table 8. Number of significant correlations (Pearson correlation coefficient) between VHI and various SPI aggregation timescales. Value is expressed as percentage evaluated with respect to the total number of grid cells (987).

	% significant correlations 5%	% significant correlations 1%
SPI1	~~94.53~~ 93.52	~~90.78~~ 91.29
SPI2	~~97.26~~ 96.76	~~95.44~~ 95.34
SPI3	~~96.66~~ 96.15	~~95.34~~ 94.83
SPI6	~~89.77~~ 90.07	~~85.61~~ 85.82

Table 9. Example of set of thresholds used to draw ROC curves for model calibration. Thresholds N and n are expressed as the percentage of the country's area instead as the number of grid cells.

	Z	z	N	n	Step of variation
Set 1	-2	varying from -1.9 to 0	25%	10%	0.1
Set 2	varying from -3.5 to -1	-1	25%	10%	0.1
Set 3	-2	-1	25%	varying from 1% to 24%	1%
Set 4	-2	-1	varying from 11% to 25%	10%	1%

Table 10. Best configuration parameters for the model when applied with PPVI, SPI3 and VHI.

	Z	z	N	n	TN	FP	FN	TP	POFD	POD
PPVI	-1.8	-1.1	~~300~~ 30%	~~80~~ 8%	957	379	99	506	0.284	0.836
SPI3	-1.3	0	20%	8%	943	393	157	448	0.294	0.749
VHI	22	40	10%	8%	935	401	150	455	0.300	0.752

Table 11. ~~performance~~ Performance of PPVI, SPI3, and VHI in identifying departments hit by drought during week 8 of 2012 and comparison with observations. Observations are retrieved from the text-based documents reported in Table 7.

Department	Reported as drought	% of the area			Ranking of affected departments		
		PPVI	SPI3	VHI	PPVI	SPI3	VHI
North West	Yes	93.1	91.7	47.2	1	1	1
Artibonite	Yes	75.1	72.8	34.1	2	7	5
North	Yes	74.6	82.1	10.4	3	4	9
Centre	Yes	67.2	54.3	45.7	4	10	2
North East	Yes	62.1	72.4	34.5	5	8	4
West	No	61.8	72.1	32.7	6	9	6
Nippes	No	51.2	75.6	36.6	7	5	3
Grand Anse	No	47.8	82.1	10.4	8	3	8
South	No	32.6	75.3	9	9	6	10
South East	No	30.8	84.6	20	10	2	7

Table 12. Drought events in Haiti according to PPVI, duration, severity and mean areal extent.

Event number	Start date	End date	Duration (months)	Mean intensity PPVI	Minimum PPVI	Mean areal extent (%)
1	22/04/1982	21/07/1983	15	-8.46	-4.73	32.13
2	27/12/1984	07/11/1985	11	-7.87	-3.91	49.60
3	18/09/1986	16/04/1987	7	-7.90	-3.62	41.65
4	16/11/1989	18/10/1990	11	-8.60	-4.59	35.48
5	07/02/1991	11/02/1993	25	-8.70	-4.69	44.92
6	16/09/1993	27/01/1994	4	-8.95	-4.48	36.98
7	11/08/1994	10/11/1994	3	-8.53	-3.50	50.11
8	20/03/1997	20/11/1997	8	-8.43	-4.32	46.00
9	30/03/2000	21/09/2000	6	-8.31	-3.79	74.07
10	30/11/2000	19/04/2001	5	-7.98	-4.75	24.58
11	09/08/2001	06/12/2001	4	-7.85	-3.52	30.23
12	04/04/2002	08/08/2002	4	-8.25	-3.47	26.20
13	19/12/2002	30/10/2003	11	-7.72	-3.44	29.31
14	15/04/2004	22/07/2004	3	-7.69	-3.37	17.89
15	02/12/2004	26/05/2005	6	-9.00	-4.40	79.00
16	23/03/2006	13/07/2006	4	-7.46	-3.43	22.97
17	21/02/2008	31/07/2008	5	-7.95	-3.78	30.07
18	17/09/2009	18/02/2010	5	-8.58	-3.95	57.48
19	21/04/2011	16/06/2011	2	-9.32	-4.14	48.28
20	29/12/2011	05/04/2012	3	-8.12	-3.91	62.52
21	19/07/2012	25/10/2012	3	-8.33	-3.62	42.16
22	07/03/2013	05/05/2016	39	-8.18	-4.00	34.50
23	29/09/2016	20/04/2017	7	-8.20	-4.06	15.02
24	12/07/2018	31/12/2018	6	-9.50	-5.58	58.50